Joana Maria de Almeida Monteiro

Impact of P-cadherin expression in the modulation of E-cadherin adhesive function in cancer cells

Dissertação de Candidatura ao grau de Mestre em Oncologia, Especialização em Oncologia Molecular, submetida ao Instituto de Ciências Biomédicas Abel Salazar da Universidade do Porto.

Orientador - Doutora Joana Paredes
Categoria - Investigadora Principal e Professora Afiliada
Afiliação - Instituto de Patologia e Imunologia Molecular
da Universidade do Porto e Faculdade de Medicina da Universidade do Porto

Co-orientador - Doutora Ana Sofia Ribeiro
Categoria – Estudante de Pós-Doutoramento
Afiliação - Instituto de Patologia e Imunologia Molecular
da Universidade do Porto

Agradecimentos

Nenhuma etapa se conquista estando sozinho, seria impossível chegar ao fim sem a ajuda de pessoas fantásticas e imprescindíveis. Obrigada a cada um deles, pela importância que teve para concluir esta etapa. Obrigada também a todas as pessoas não referidas, que de algum modo possam ter sido importantes.

À Joana, pela oportunidade para integrar esta equipa fantástica que tanto me fez crescer e aprender. Pelos conhecimentos, sabedoria, ajuda e boa disposição. Que nunca percas o espírito que caracteriza este grupo.

À Ana Sofia, obrigada por tudo o que pude aprender contigo, pela simpatia e energia positiva que tens sempre. Por toda a ajuda e apoio, pela paciência para os erros e disparates. Por veres sempre o lado positivo das situações, mesmo quando parece impossível existir. Muito, muito obrigada por tudo.

Ao grupo “da mama”, pela ajuda tanto nos mais insignificantes pormenores, como pela ajuda a crescer como pessoa. Foi muito bom partilhar com vocês estes meses de erros e aprendizagens.

Ao professor Nuno Santos e à Filomena, por toda a ajuda no tempo que estive no IMM. Pela sabedoria, conhecimentos e apoio, não poderia ter sido mais bem recebida. Obrigada por todo o tempos despendido comigo e com os meus resultados, sem dúvida que sem vocês não teria sido possível.

Aos meus pais, por tudo! Por estarem sempre presentes mesmo nas escolhas erradas, por não desistirem mesmo se eu quisesse desistir, pelo sorriso, abraço, carinho e porto-seguro que só eles sabem ser e dar. Na esperança que se orgulhem de mim, tanto como eu me orgulho deles.

À minha família por toda a ajuda, compreensão e afecto. Em especial aos meus avós pela estadia e mimos nos meses que estive em Lisboa. À minha avó, pelos mimos de fim-de-semana.

À Filipa, minha eterna colega de jornada, um grande obrigada por tudo. Obrigada por me ouvires, por me ajudares SEMPRE. Obrigada por todo o apoio, confiança, ajuda, sorrisos e brincadeiras. Contigo foi muito mais fácil. E principalmente obrigada por me teres deixado conhecer-te!

À Inês, recente aquisição de colega de casa. Obrigada pelas pausas, devaneios a conversas de café no quarto. Obrigada por teres acreditado em mim, por ajudares nas dúvidas existenciais, e por partilhares gelado e chocolate comigo. És mais forte do que pensas.

À Cristina, por toda a energia positiva, pausas e apoio. Por ajudares a ver sempre o lado positivo das situações, por seres a mais bem-disposta. Por nunca teres falhado em nada.

À Filipa, pelo tempo que perdeste comigo, por tudo o que me ensinaste e pela paciência que tiveste comigo por terras Lisboetas, obrigada!

À Ana, pelas noites que passaste a ouvir-me, pelas opiniões sinceras, apoio e ajuda. Por aturares o mau feitio em casa e por ajudares a descontrair. E ao Xavier por ser a bola de pelo mais fofa e gorda de sempre.

Às Sacaninhas, Ro, Mara, Chica, Bela e Tixa pelas loucuras, jantares, companheirismo, festas, filmes, conversas e tudo mais. Sem vocês não teria o mesmo sabor.

À Joana Marta, por estares comigo desde que me lembro que existo. Pelos desabafos, conversas sem nexo, cafés e bailaricos de fim-de-semana. Por seres a única, desde sempre.

Ao Jorge, Sérgio, Mariana, Joel, Dirce, Bruno, Ana Marta, às afilhadas Diana e Kika, por me apoiarem sempre e fazerem sorrir mesmo nos momentos mais difíceis. Pelas parvoíces. “Amigos são a família que escolhemos.”

Ao André, pelo apoio e por ouvir todas as queixas possíveis e imaginárias. Pelos risos e sorrisos, obrigada. Por acreditares em mim nos melhores e piores momentos, por seres o melhor amigo que poderia ter.

Ao Ruca, o mais fiel dos companheiros. “All his life he tried to be a good person. Many times, however, he failed. For after all, he was only human. He wasn't a dog.”

Abstract

Tumourigenesis and progression to metastasis are promoted by the disequilibrium in cellular physical and chemical forces that are able to regulate proliferation, differentiation and migration. It is already assumed that structural changes in the binding to the extracellular matrix, as well as in the cell cytoskeleton are, at a molecular level, responsible by tumour initiation and progression. During disease, it is known that cells change their physical properties. Cell-cell adhesion, namely the one promoted by cadherins, has a crucial role in these processes, since they serve to mechanically couple cells. In response to external forces, cells may stiffen, change their shape or alter their behavior, including their gene expression profile. These changes involve multiple signaling pathways and many of the responses ultimately affect the actin cytoskeleton.

E- and P-cadherin belong to the classical cadherin family of proteins and interact intracellularly with the catenins family of proteins. E-cadherin is a growth and invasion suppressor, and its loss of function is a prerequisite for tumour invasion and metastasis formation. On the other hand, P-cadherin has been shown to be overexpressed in several solid tumors, including breast cancer, being associated with carcinomas of high histological grade and poor patient survival. Recently, our group has described P-cadherin has a breast cancer stem cell marker, with a key role in some acquired cancer hallmarks, since its overexpression promotes *in vitro* cell migration and invasion of breast cancer cells. We demonstrated that P-cadherin *in vitro* effects are due to inhibition of the E-cadherin suppressive invasive function, by disruption of the E-cadherin/p120catenin complex at the cell membrane. Recently, we still found that P-cadherin-induced invasion is dependent on Src-activity, which regulates the expression and trafficking of E-cadherin. In breast cancer, the increased activity of Src has been correlated with an invasive cell phenotype and metastatic disease, demonstrating that Src might promote these alterations through its capacity to modulate cell-cell and cell-matrix adhesive interactions in tumour cells.

Taking that into account, we hypothesized that P-cadherin could alter the morphological and biomechanical properties of breast cancer cells through Src activation, and these alterations would underlie the invasive and tumorigenic phenotype of P-cadherin overexpressing cells. If true, these alterations in the mechanical properties of cancer cells could also be used as biomarkers in early detection of cancer, as well as to the response to anti-cancer drug efficacy tests.

Thus, in order to evaluate the biomechanical properties induced by P-cadherin expression, we have used atomic force microscopy (AFM), which is a method for high-

resolution imaging of any surface, for characterization of mechanical, electrical and magnetic characteristics of samples. Two different breast cancer cell models were used (MCF-7/AZ and BT20), where P-cadherin expression was manipulated. By AFM, we found that P-cadherin overexpressing cells present significantly higher area and volume, as well as a decrease height, when compared with cells with lower levels of P-cadherin. Additionally, overexpression of P-cadherin in breast cancer cells presented a lower Young's Modulus, which indicates higher cell elasticity; accordingly, P-cadherin silencing in BT-20 cells induced a significant increase in the Young's Modulus value, revealing a decreased elasticity. Regarding cell-cell adhesion, the Work needed to disaggregate P-cadherin overexpressing cells was lower than in the controls, indicating that in the presence of P-cadherin expression is easier to separate tumour cells. Interestingly, the treatment of P-cadherin-overexpressing cells with Dasatinib, a highly potent Src kinase inhibitor with antiproliferative activity, induced the same results in both models: a reduction in the cell's area and volume, as well as an increase in the cellular height and Young's Modulus (less elastic cells). Concerning cell-cell adhesion, we found that the work required to separate P-cadherin overexpressing cells was significantly higher after Dasatinib treatment.

Our results show, for the first time, that P-cadherin overexpression, in an E-cadherin wild-type context, turns cells more flat, more elastic and less cohesive. AFM measurements demonstrated that P-cadherin repressed the normal cell-cell adhesion mediated by E-cadherin in cancer cells, correlating well with its role in breast cancer cell invasion and migration. In addition, we also showed that Dasatinib treatment is able to revert the P-cadherin-induced morphological and biomechanical changes.

In conclusion, this study contributed to clarify the role of P-cadherin expression in the biomechanical properties of breast cancer cells. Moreover, it showed how AFM can be an essential tool to study these morphological and mechanical alterations, and how these correlate so well with tumour cell's behaviour.

This work reinforced the importance of P-cadherin expression as a prognostic factor for breast cancer patients and supports the development of new therapeutics to control aggressive carcinomas co-expressing both epithelial cadherins.

Resumo

Os processos de tumorigénese e metastização são promovidos pelo desequilíbrio nas forças físicas e químicas das células tumorais, que permitem regular proliferação, diferenciação e migração. Existem várias publicações que demonstram que alterações estruturais na ligação à matriz extracelular, assim como no citosqueleto de uma célula são, a nível molecular, responsáveis pela iniciação e progressão tumoral.

A adesão célula-célula, nomeadamente a desempenhada pelas caderinas, tem um papel crucial nesse processo, uma vez que unem as células mecanicamente. Em resposta a forças externas, as células podem endurecer, alterar a sua forma ou alterar o seu comportamento, incluindo o próprio perfil de expressão génica. Estas alterações envolvem várias vias de sinalização, e muitas das respostas afectam o citoesqueleto.

As caderinas-E e -P pertencem à família das caderinas clássicas de proteínas e interagem intracelularmente com proteínas da família das cateninas. A caderina-E é supressor de invasão e crescimento, e a sua perda de função é um pré-requisito para a invasão tumoral e formação de metástases. Por outro lado, foi demonstrado que existe sobrexpressão de caderina-P em inúmeros tumores sólidos, incluindo cancro da mama, sendo associado a carcinomas de alto grau histológico e a um mau progóstico. Recentemente, descrevemos a caderina-P como um marcador de células estaminais de cancro da mama, tendo um papel crucial na indução de migração e invasão celular. Demonstrámos ainda que os efeitos *in vitro* da caderina-P se devem à inibição da função supressora de invasão da caderina-E, através da disrupção do complexo membranar caderina-E/p120-catenina. Recentemente, verificámos que a invasão induzida pela caderina-P é dependente da atividade da Src, que regula a expressão e o tráfico da caderina-E. No cancro da mama, o aumento da atividade da Src tem sido correlacionada com um fenótipo celular invasivo e com doença metastática, demonstrando que a Src pode promover essas alterações através da sua capacidade para modular interações célula-célula e célula-matriz em células tumorais.

Tendo isso em conta, colocamos a hipótese de que a caderina-P poderia alterar as propriedades morfológicas e biomecânicas das células de cancro da mama através da ativação da Src, e que essas alterações estariam subjacentes ao fenótipo invasivo e tumorigénico das células que sobrexpressam caderina-P. Estas alterações nas propriedades mecânicas em células cancerígenas podem também ser utilizadas como biomarcadores na detecção precoce de cancro, assim como em testes eficazes de drogas anti-tumorais.

Assim, para avaliar as propriedades biomecânicas induzidas pela expressão de caderina-P, usámos microscopia de força atómica (AFM), que é um método de imagem de elevada resolução de qualquer superfície, que caracteriza amostras do ponto de vista mecânico, elétrico e magnético. Dois modelos celulares de cancro da mama foram usados (MCF-7/AZ e BT20), em que a expressão de caderina-P foi manipulada. Por AFM, demonstrámos que células com sobrexpressão de caderina-P apresentam volume e área significativamente superior, assim como uma diminuição na altura, quando comparadas com células com baixa expressão de caderina-P. Além disso, a sobrexpressão de caderina-P em células de cancro da mama levou a uma diminuição do *Young's modulus*, indicando uma maior elasticidade celular, enquanto que o silenciamento da caderina-P nas células BT20 induz um aumento significativo do valor de Young's modulus, revelando uma diminuição da elasticidade. Relativamente à adesão célula-célula, o trabalho necessário para desagregar células que sobrexpressam caderina-P foi menor em relação ao controlo, mostrando que na presença de expressão de caderina-P é mais fácil separar células tumorais.

Curiosamente, o tratamento de células com sobrexpressão de caderina-P com Dasatinib, um potente inibidor da Src kinase com atividade anti-proliferativa, induz os mesmo resultados em ambos os modelos: uma redução no volume e área celular, assim como um aumento na altura e no valor de Young's modulus (células menos elásticas). Em relação à adesão célula-célula, o trabalho necessário para separar células com sobrexpressão de caderina-P foi significativamente maios após o tratamento com Dasatinib.

Os nossos resultados mostram, pela primeira vez, que a sobrexpressão de caderina-P, num contexto normal de caderina-E, torna a célula mais plana e elástica e menos aderente. As medidas de AFM demonstram que a caderina-P reprime a adesão normal célula-célula mediada pela caderina-E em células tumorais, estando estas correlacionadas com o seu papel na invasão e migração de células de cancro da mama. Demonstrámos ainda que o tratamento com Dasatinib reverte as alterações morfológicas e biomecânicas induzidas pela caderina-P.

Em conclusão, este estudo contribuiu para clarificar o papel da expressão da caderina-P nas propriedades biomecânicas das células de cancro da mama. Além disso, mostrou como o AFM pode ser uma ferramenta essencial para estudar essas alterações morfológicas e mecânicas, e como se relacionam com o comportamento de células tumorais.

Este trabalho reforça a importância da expressão da caderina-P como um factor de prognostico para doentes com cancro da mama, e apoia o desenvolvimento de novas

terapias para controlar carcinomas agressivos com co-expressão de ambas caderinas epiteliais.

.

Table of contents

Abreviation List

Abl	Abelson leukemia virus
AFM	Atomic force microscopy
BCR	Breakpoint cluster region
Ca^{2+}	Calcium
CBD	Catenin-binding domain
CML	Chronic myeloid leukaemia
EC	Extracellular domain
EGFR	Epidermal growth factor receptor
EMT	Epithelial to mesenchymal transition
ER	Oestrogen receptor
FA	Focal adhesions
FAK	Focal adhesion kinase
FGFR	Fibroblast growth factor receptor
HER2	Human epidermal growth factor receptor 2
IL-8	Interleukin 8
JMD	Juxtamembrane domain
KO	Knockout mice
MAPK	Mitogen activated kinase
MMPs	Matrix metalloproteases
Myr	14-carbon myristic acid moiety
PBS	Phosphate buffered saline
Ph+ ALL	Philadelphia chromosome-positive acute lymphoblastic leukemia
Rac1	Ras-related C3 botulinum toxin substrate
Ras	Rat sarcoma viral oncogene
SFKs	Src family kinases
SH	Src homology domain
siRNA	Small interfering RNA
VEGF	Vascular endothelial growth factor
VEGFR	Vascular endothelial growth factor receptor

Hz	Hertz
kHz	Kilohertz
mm	Millimetres
N	Newton
N/m	Newton / meter
nm	Nanometre
Pa	Pascal
pN	Piconewton
µg/ml	Microgram per milliliter
µL	Microliter
µm	Micrometre
kPa	Kilopascal
J	Joules

List of Figures

INTRODUCTION

1. Classical epithelial cadherins

1.1. E-cadherin and P-cadherin

I. Structure and function

Classical cadherins are glycoproteins that mediate calcium-dependent cell-cell adhesion in solid tissues, existing in vertebrates as well as in invertebrates (1). They are usually localized on the surface of epithelial tissues, in regions where the cell-cell adhesion takes place, called adherens junctions (2).

Epithelial-cadherin (*E-cadherin*) and Placental-cadherin (*P-cadherin*) constitute the classical epithelial cadherins, since they are expressed in all epithelial tissues, sharing a common structural component (3). *CDH1* and *CDH3* are the genes that encode epithelial cadherins, E- and P-cadherin respectively, which are present in the human chromosome 16q22.1; *CDH3* is 32kb upstream *CDH1*, and they have 66% of homology (1).

E- and P-cadherins are constituted by an extracellular domain, a single transmembrane domain and a cytoplasmic domain. The extra-cellular domain is constituted by five cadherin repeats (EC1-EC5), which are sequences of 110 residues that are present only in classical cadherins family. The presence of calcium (Ca^{2+}) is responsible for the conformation of cadherins, which only stabilize in its presence, turning their structure more rigid. Calcium-binding sites are constituted by short highly conserved amino acid sequences, localized between successive EC domains (2). The homophilic affinity of cadherins form homodimers that establish the adhesion between two adjacent cells. This affinity is possible due to the 40 amino acid residues that are located in the C-terminal region of EC1 (4). There are some reports that show that there are heterophilic interactions between cadherins (5), being however these interactions weaker than the respective homophilic counterparts (6).

Concerning the cytoplasmic domain, it is divided in two subdomains: the juxtamembrane domain (JMD) for p120ctn and the catenin-binding domain (CBD) for β-catenin or γ-catenin binding (2), forming the cadherin-catenin complex, responsible for normal cell‑cell adhesion and homeostatic tissue architecture. β-catenin and γ-catenin bind directly to α-catenin (1), which links the cadherin-catenin complex to the actin cytoskeleton, to promote strong cell-cell adhesion (1). The number of cadherins present in the different cells, as well as distinct landscapes of their structure, allows precise temporal and spatial transcriptional regulation of the different subtypes. Variations in protein structure, namely in the cytoplasmic domain, simplify interactions that result in both specific modulation of cadherin activity an initiation of intracellular signalling cascades in response to adhesion (7).

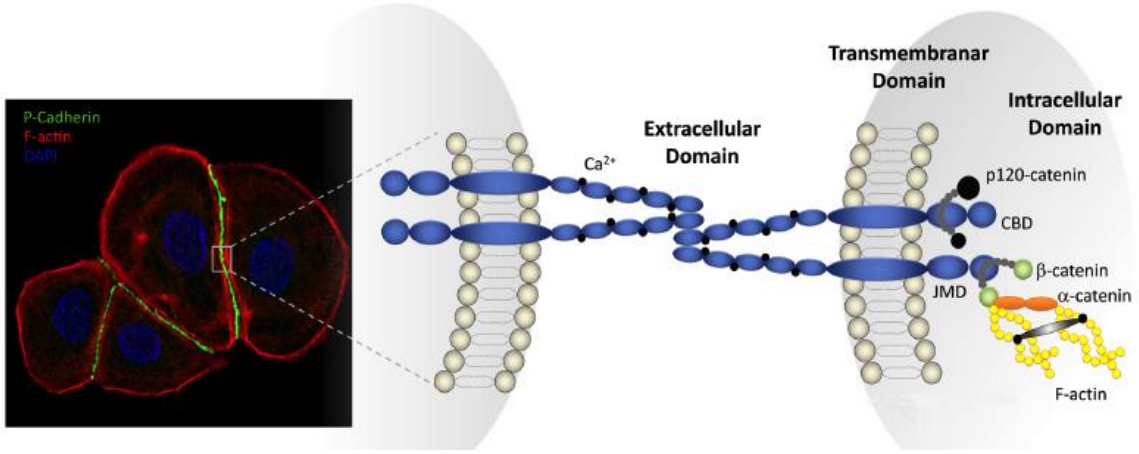

Figure 1 - Schematic representation of the structural components of the P-cadherin adhesive junction. Lateral clustering of P-cadherin molecules is required to form stable cell-to-cell contacts in BT-20 breast cancer cells [immunofluorescence: P-cadherin (green), F-actin (red), DAPI (blue)]. In the intercellular space, P-cadherin extracellular domains interact with P-cadherin extracellular domains of adjacent cells to mediate cell adhesion. The intracellular catenins bind to the cytoplasmic tail of P-cadherin. p120-catenin binds the cadherin tail at the juxtamembrane domain (JMD), whereas b-catenin binds to the distal catenin binding domain (CBD). α-catenin associates with beta-catenin and is directly linked to the actin cytoskeleton. Adapted from Albergaria A, 2011 (9).

A decrease in gene transcription of E-cadherin results in loss of cell-cell adhesion and increased cell migration. Transport of E-cadherin newly synthesized to plasma membrane requires the bind of β-catenin and, once provided to the cell surface, E-cadherin is regulated by phosphorylation, ubiquitination and proteolysis (7).

II. Cadherin/catenin complex and actin cytoskeleton

Adhesion forces that are established by cadherins and catenins are named adheren junctions and are formed by complex and highly dynamic interactions. The members of cadherin's family make this connection with members of the armadillo repeat protein superfamily: p120-catenin and β-catenin, as well as with α-catenin, structurally unrelated and lacking armadillo domains (8). The function and strength of cadherin-mediated adhesion depends on its dynamic association with catenins, which link the cadherin cytoplasmic tail to the actin cytoskeleton and facilitate clustering into the junctional structure, forming cadherin/catenin complexes (9). P120-catenin acts to stabilize cadherins at the cell surface and may control regulators of the actin cytoskeleton and the rate of cadherin endocytosis (10). On the other side, β-catenin has an important role on the maintenance of the cytoskeleton structure, since it makes the link with α-catenin, which afford a functional connection with the actin cytoskeleton, stabilizing the cell-cell adhesion (11). The binding of α-catenin to actin filaments and β-catenin is

mutually exclusive, which turns impossible the direct link between cadherins and the actin cytoskeleton.

The structural integrity of the cadherin-catenin complex is regulated by phosphorylation, positively and negatively. If by one hand, phosphorylation of three serine residues in the E-cadherin cytoplasmic domain generates additional interactions with β-catenin, causing an increase in the affinity between these two proteins, on the other hand, tyrosine phosphorylation of β-catenin disrupts the binding with E-cadherin or α-catenin. These phosphorylations are balanced by protein tyrosine phosphatases, which stabilize cadherin/catenins interactions (7).

Adheren junctions have the function to maintain the correct functioning of cell-cell adhesion and to ensure cell and tissue morphology and structure, acting as suppressors of tumour invasion (12, 13). Modifying the structure of the cadherin-catenin complex can have a crucial impact not only on cell-cell adhesion, but also in cell signalling. Interfering with this complex, may promote delocalization of the catenin family proteins from the cell membrane to the cytoplasm, where these molecules can activate several signalling pathways. Free cytoplasmic β-catenin is responsible for activation of the Wnt-signalling pathway. Moreover, p120-catenin may activate indirectly Rac1 and Cdc42 and may regulate the cadherin-actin cytoskeleton link directly by binding and inhibiting RhoA (4).

III. Role in normal development and tissue differentiation

E-cadherin is a growth and invasion suppressor, expressed mainly in epithelial cells in normal tissues. Instead, P-cadherin also contributes to cell-to-cell adhesion, but its expression is restricted to specific areas of epithelial tissues, normally proliferating regions, co-localising partially with the expression of E-cadherin (1). But the role of cadherins is not limited to mechanical adhesion, extending their functions to tissue morphogenesis, cell recognition and sorting, boundary formation and maintenance, coordinated cell movements, induction and preservation of structural and functional cell tissue and polarity. Distinct cadherin subtypes lead to the differentiation of specific tissues and perhaps supress the differentiation of others (7).

Both E- and P-cadherin were described as important proteins to ensure the cell-cell and cell-matrix adhesion in development of embryos. E-cadherin was shown to be present in the stage of one cell of the embryo, but also in posteriors stages, like the 8-cell stage, being essential for the morula compaction and organization of epithelial tissues. After that, the embryo implantation in uterus involves E- and P-cadherin. During development, it seems that these cadherins show complementary and opposite functions, because E-cadherin is expressed only in embryonic region of placenta, whereas P-cadherin is expressed both in embryonic and maternal placenta. The first one is important

for preventing the mixture of tissues and the second one, is essential for assembly the association and recognition of both tissues (9). Each subtype of cadherin tends to be expressed at the highest levels in different tissues during development. E-cadherin, in addition to being present at the morula stage, is expressed in all ephitelia, whereas P-cadherin is present in the basal layer of epithelial tissues.

However, it is not only in the embryo development that cadherins assume functions. They have been also linked with the formation and maintenance of diverse tissues and organs, as the polarization of simple epithelia, the mechanical linking of hair cells in the cochlea and supplying the adhesion code for neural circuit formation during wiring of the brain. In adult tissues, E-cadherin is important for the foundation, maintenance and homeostasis of epithelia. The principal function is the establishment of adherens junctions, responsible for cell-cell adhesion in a high number of tissues. E-cadherin also plays an important role in cell polarity establishment, spatially confining signalling molecules, specifying the plane of cell division, regulating cell division along one axis and allowing directional expansion of tissues (7).

E- and P-cadherin have an important role to normal development as demonstrated by gene knockout mice (KO). E-cadherin KO is lethal at early stages of mouse embryogenesis, due to the failure of trophoectoderm formation, the first polarised epithelial layer in this model (14). On the other hand, loss of function of P-cadherin is not lethal. However, it is associated to development defects, namely of the breast. Deletion of P-cadherin affects normal mammopoiesis, since the *CDH3*-null female mice exhibit precocious mammary gland differentiation in the virgin state, and breast hyperplasia and dysplasia with age. These observations indicate that P-cadherin-mediated adhesion, or signals derived from its cell–cell interactions, are indeed important determinants of mammary gland growth control and in the maintenance of an undifferentiated state during a specific period of time (1).

1.2. Epithelial Cadherins in cancer cell invasion and motility

E-cadherin is an important invasion suppressor protein, and it is known that its loss of expression and/or abnormal function leads to an increment of the ability to invade adjacent tissues, like in cancer invasion. Instead, the expression of P-cadherin is correlated with cell differentiation and proliferation and with connection of epithelial cell layers (1). Most common tumours are carcinomas, which derivate from epithelial tissues, being E-cadherin the prototypical cadherin, responsible for inducing cell polarity and organization of epithelium. As tumours progress towards malignancy, lose partially or completely E-cadherin-mediated cell-cell adhesion (15). Loss of E-cadherin-mediated cell-

cell adhesion is a prerequisite for tumour invasion and metastasis formation. Reversion of this lost, re-establishing the cadherin/catenin complex, results in a reversion from an invasive and mesenchymal phenotype to a benign and epithelial phenotype of culture cell lines (16).

Loss of E-cadherin function during tumour progression can be lead by diverse genetic or epigenetic mechanisms. The most common alteration is the deregulation at the transcriptional level. Proteins like Snail and Slug, transcriptional repressors, actively links to the promoter of E-cadherin, repressing its expression (17). Transcriptional inactivation of E-cadherin leads consequently to epigenetically silencing of E-cadherin gene locus, resulting in additional downregulation of its expression (18). Another mechanism responsible for ablation of cell-cell adhesion mediated by E-cadherin is the proteolytic degradation of this protein by matrix metalloproteases (MMPs). In consequence of this degradation, a soluble 80-kDa form of E-cadherin is found in cultured tumour cell lines and also in tumour biopsies. This soluble product promotes tumour-cell invasion, upregulating MMPs (19).

Contrarily to E-cadherin, P-cadherin seemed to be frequently up-regulated in tumours, being reduced when tumour cells are more differentiated. P-cadherin has been shown to be overexpressed in several solid tumors, including breast, prostate, colon, pancreatic and bladder cancer (20). Besides being altered in various human tumours, P-cadherin role in carcinogenesis process remains unclear since, depending on the studied tumour cell model and context, it behaves in a different manner. In melanomas, P-cadherin behaves as an invasion suppressor gene, since in highly invasive melanoma cell lines, without E-cadherin expression, P-cadherin overexpression was able to promote the formation of cell-cell interactions and counteract invasion (9, 21). On the other hand, in other models, including breast cancer, P-cadherin behaves as an oncogene, being reported to correlate with increased tumour cell motility and invasiveness when aberrantly expressed (22). The role of exogenous P-cadherin was for the first time demonstrated in a study using *in vitro* cell models, where was found that its overexpression is able to promote single cell motility, inducing an increase in the number of moving cells and speed, when comparing with cells with low levels of cadherins. Besides that, P-cadherin is also able to induce phenotypic changes involving alterations in cell polarity and leading edge morphology, formation of membrane protrusions and increase of their cytoplasmic area, characteristics from cells with a motile behaviour (23).

It was also demonstrated that P-cadherin *in vitro* effects are due to inhibition of the E-cadherin suppressive invasive function, by disruption of the E-cadherin/p120catenin complex at the cell membrane (6).

Considering this important role of P-cadherin in tumor progression, a humanized monoclonal antibody (PF-03732010) was developed to antagonize P-cadherin-regulated cell-cell adhesion and the associated signaling pathway. A study using this antibody confirmed the role of P-cadherin as a molecule involved in cell invasion and metastization. The authors observed that PF-03732010 treated cells and tumors showed disrupted P-cadherin signaling and resulted in an anti-metastatic, anti-proliferative activity and in the induction of apoptosis (24).

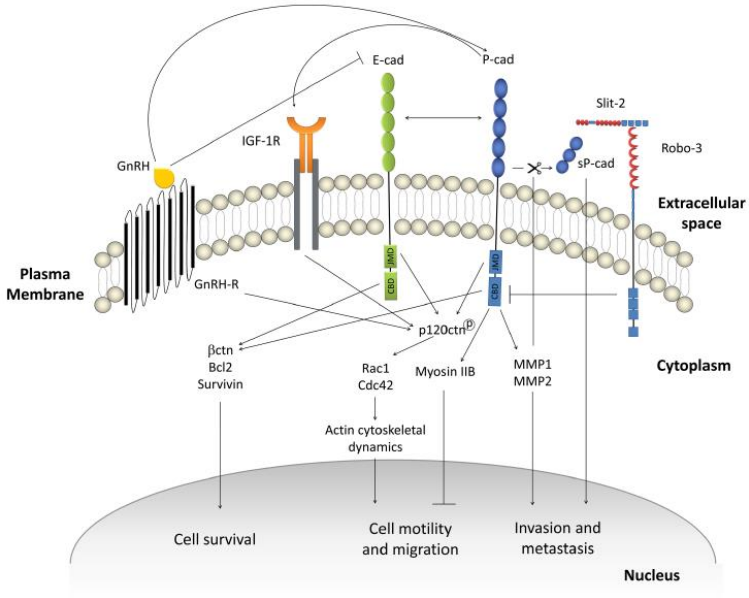

Figure 2 -Schematic representation of the signalling pathways regulated by P-cadherin expression. P-cadherin signals are transduced by many intracellular signalling pathways, which ultimately result in alterations of the cancer cells survival, as well as cell migration and invasion capacity. For simplicity, only some of the known interactions are depicted. It should be noted that the effect of P-cadherin on the overall gene expression program of cancer cells is highly dependent on the cellular type and the biological context. Adapted from Albergaria A, 2011 (9).

1.3. Epithelial Cadherins in Breast cancer

The tumour suppressor role of E-cadherin has a particular interest in breast cancer, due to the high frequency of loss of heterozygosity (more than 50%) in chromosome region 16q22.1, where is located the *CDH1* gene responsible for encoding this protein (25). Loss of E-cadherin is one of the main phenotypic characteristics of

invasive lobular breast carcinoma, found in more than 85% of these lesions, described by prominent single cell infiltration. Loss of heterozygosity combined with *CDH1* mutations is present in close to 50% of invasive lobular breast cancers. Ductal breast carcinomas present loss of heterozigosity in close to 50% of the cases, lacking mutations in the remaining CDH1 allele and displaying high variability of E-cadherin expression. Reduction of E-cadherin levels are due to epigenetic silencing via promoter hypermethylation or transcriptional repression (26). Immunohistochemistry studies usually associate loss of E-cadherin in advanced stages of breast cancer, supporting the view that loss of E-cadherin expression is a marker of aggressiveness. Nonetheless, most of the times, there is no correlation between E-cadherin and other prognostic parameters, such as tumor size, tumor grade, ER, PR and HER-2 expression. Indeed, in the last years some reports claim no alterations in E-cadherin expression in breast cancer progression. The persistence of E-cadherin expression in high grade tumors and large size tumors contrasts with most of the reports of E-cadherin in breast cancer, which have described down regulation of this molecule during tumorigenesis. In fact, the mouse 4T1 breast cancer cell line, which is a clinically relevant model of spontaneous metastasis, expresses high levels of E-cadherin (27, 28), as does the inflammatory breast cancer, one of the most aggressive human cancers (29, 30). Also, derivative metastases frequently show strong E-cadherin expression (31), as well as staining of E-cadherin may persist into late stages of breast carcinoma, though it may be functionally inactivated (32, 33).

In what concerns P-cadherin it seems to have an opposite function to what has been observed for E-cadherin. Indeed, P-cadherin was reported as a marker of poor prognosis in breast cancer, since P-cadherin-positive carcinomas were significantly associated with short-term overall and disease-specific survival, as well as with distant and loco-regional relapse-free internal (34, 35). P-cadherin is one of the markers expressed by a subset of breast tumors with a worse prognosis to the patients, the basal-like tumors. We and others have also reported that P-cadherin expression was inversely related to hormonal receptor content (the majority of the cases were negative for ER and PgR) (22, 34-40) and directly related to the expression of the epithelial growth factor receptor (36), HER2, p53 expression, high proliferation rates (MIB-1), mitotic index and decreased cell differentiation, which are biological conditions with strong associations with poor survival of breast cancer patients (34, 35, 40). However, P-cadherin expression partially overlaps with E-cadherin expression, being its cancer-related function context dependent (41). Expression of P-cadherin associated with tumourigenesis is present in various epithelial tumours types, but specially more in invasive lesions than in *in situ* lesions (1). Tumours that co-express both E- and P-cadherin, presents cytoplasmic activation of p120-catenin, which is also correlated with poor patient survival (42).

During breast cancer progression, P-cadherin is overexpressed and is associated with worse patient survival, however the cellular mechanism responsible from this remained elusive. E- and P-cadherin co-expression possibly could be involved in a more aggressive biological behaviour of breast cancer cells, due to interaction of both molecules at the cellular membrane, interfering with the establishment of a strong adhesion complex. Regarding cell models with expression of both E- and P-cadherin, there is a deregulation in cadherin/catenin complex at the cellular membrane, contrarily cells that only express one of the cadherins showed an increase in these interactions. Thus, E- and P-cadherin heterodimers are not efficient in the stabilization of a strong cadherin/catenin complex at the cellular membrane, showing the cells an aberrant behaviour (43). P-cadherin has function of an invasive suppressor when it is the only cadherin present in the membrane, because in co-expression of E-cadherin has a pro-invasive function. Moreover, simultaneous expression of cadherins promotes aggressive biological behaviour and different gene expression profiles. This explains the poor prognosis of patients with tumours that co-express both cadherins (43, 44).

2. Src family tyrosine kinases

2.1. Src signaling

Src (or c-src) was the first oncogene described. It was defined as the main responsible for the release of a sarcoma-causing virus (Rous sarcoma virus) in chickens, and called in that time, v-src, having won this discovery a Nobel Prize. Src was also the first protein described as to have an intrinsic protein tyrosine kinase activity (12) (45).

Localized in the intracellular membrane of the cells, Src family kinases (SFKs) are constituted by 11 nonreceptor tyrosine kinases, namely Src, Fyn, Yes, Blk, Yrk, Frk (also known as Rak), Fgr, Hck, Lck, Srm and Lyn. These proteins are expressed in a variety of tissues, like keratinocytes, bladder, breast, brain, colon and lymphoid cells (45). SFKs have a molecular weight between 52 and 62 KDa and are composed by 6 functional regions: a 14-carbon myristic acid moiety (Myr) attached to the Src homology domain 4 (SH4), a unique region constituted by an SH3 and an SH2 domain (both related with interactions with other proteins), an SH2 kinase linker, an SH1 domain which contains Tyr419 (the phosphorylation in this residue is required for maximum kinase activity) and a C-terminal domain containing Tyr530, acting as a negative regulatory domain (46, 47).

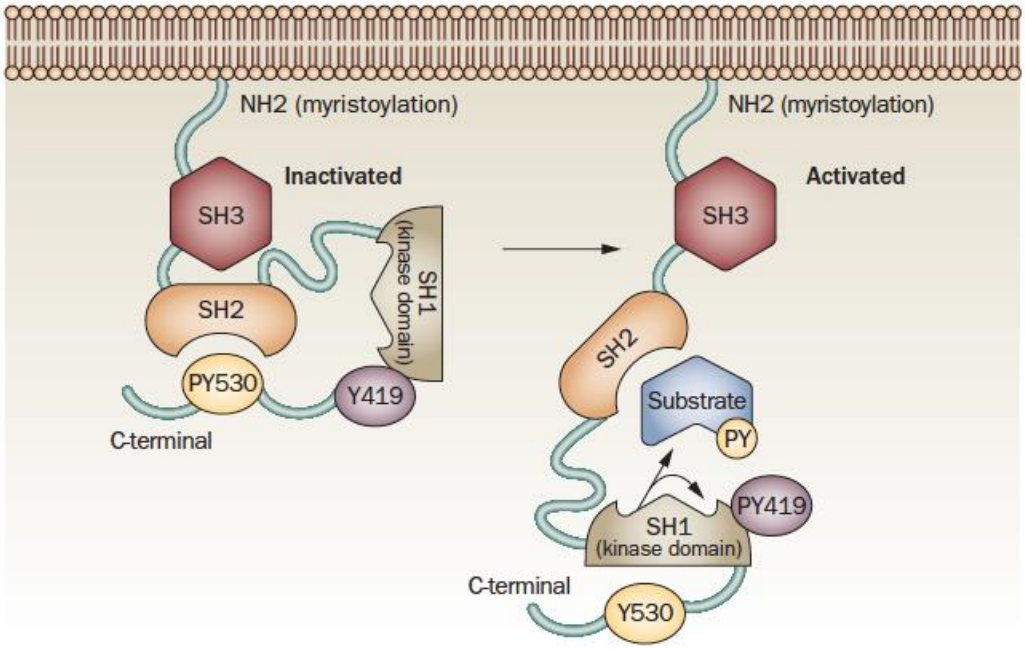

Figure 2 - Structure and activation of Src. The Src protein is composed of four Src homology domains (SH1, SH2, SH3, and SH4). The SH4 is located on the N-terminal region and contains a myristoylation sequence important for membrane attachment. The SH3 domain is a proline-rich target domain that binds and interacts with other proteins or with Src itself. The SH2 domain can recognize phosphorylated tyrosine containing residues, critical for regulation of Src activity or binding to other tyrosine proteins. The SH2-linker, located between SH2 and SH1, can regulate Src activity and interact with SH3. The SH1 domain contains the kinase domain as well as tyrosine residue Tyr419, which is phosphorylated by the kinase domain. Adapted from Kim L. C., 2009 (46).

Activation and inactivation of c-Src is attended by conformational changes in the protein. These alterations can be affected by several factors, like SH2-binding and SH3-binding ligands, activation of the catalytic domain or dephosphorylation of the C-terminal region at Tyr530. When inactivated, the SH2 domain recognizes and binds to the phosphorylated Tyr530 residue of the C-terminal of c-Src, preventing interaction of substrate proteins with the kinase domain (47, 48).

Functionally, SFKs regulate intracellular signalling pathways, through SH2 domain and trigger a cascade of downstream signalling, activating transmembrane growth factors and cytokine receptors, like VEGFR, HER2, and EGFR. c-Src encodes a non-receptor tyrosine kinase, that when activated, leads to cell proliferation, adhesion, survival, differentiation, invasion and migration in numerous biological models. When SFKs expression is altered or deregulated can be associated with cancer development and progression. There are several studies that demonstrate the role of SFKs catalytic activity in tumorigenesis of diverse type of cancers, such as breast, colorectal, prostatic, melanoma, gastric and ovarian cancers (49).

Adherens junctions can be damage by loss or defective effects of SFKs, suggesting that those kinases are critical signalling proteins for the regulation of adherens junction network. Constitutively activated Src can phosphorylate cadherins, leading to a loss of cadherin-catenin complex function, promoting cell differentiation, migration and invasiveness (50, 51). This suggests that Src can be critical in mediating epithelial-mesenchymal transition and tumour metastasis (47, 52).

2.2.Functions in breast cancer

In human tumours, mutations, amplifications or rearrangements of Src are rare, suggesting that SFK activation may be more critical for tumour progression than tumour initiation (53). Src has been found overexpressed or highly activated in a various number of tumours, as carcinomas of the breast, lung, colon, cervix, skin and gastric, neuroblastomas and myeloproliferative disorders (54). Elevated Src activity in cell lines and tumour tissues is correlated with an invasive cell phenotype and metastatic disease, demonstrating that Src might promote these alterations through its capacity to modulate cell-cell and cell-matrix adhesive interactions in tumour cells (12). Specifically, in breast cancer, the increased activity of c-Src has been associated with tumour initiation, progression and metastasis (49).

Several studies aiming to clarify the main mechanisms responsible for the invasive phenotype in a number of endocrine and anti-growth factor resistance *in vitro* models, have identified increased Src activity, which could explain the anti-hormone resistance in breast cancer cells (55). It is uncertain which is the mechanism responsible for the elevated activity of Src in anti-hormone resistant cells. There are several hypotheses to explain that activity, including alterations in the activity of regulatory phosphatases or kinases that control Src phosphorylation, activation of growth factors signalling pathways and to the shift of negative-intramolecular SH-binding interactions in the Src protein through its binding to substrates such as growth factor receptors (12, 54, 56, 57). These remarks suggest that the increase in Src activity that is observed in anti-hormone resistant tumours is due to multiple causes, including variations in one or more regulatory elements.

Src can interact with a huge number of important elements in cancer development, such as growth factor, steroid and cell-cell adhesion receptors and integrins (12). In breast cancer, Src and EGFR overexpression can be responsible for EGFR inhibitor resistance, due to the formation of a plasma membrane-associated complex between them, promoting the development and progression of tumours. Elevate activity of Src mediates signalling by growth factor receptors, including EGFR, Her2 and oestrogen receptor (ER), also contributing to endocrine therapy and Her2 inhibition resistance (58). On the other hand, Src can phosphorylate EGFR and this process is essential for the mitogenic downstream signalling instigated by EGFR (59). SFK control multiple cell functions in cancer development, including cell cycle progression, survival and metastasis and Src overexpression in breast cancer is implicated in tumour aggressiveness (45, 60).

Constitutively activated c-Src can phosphorylate E-cadherin. It is known that during tumour development, loss of E-cadherin function in epithelial cells results in an enhanced invasive and metastatic capability. This src-mediated-phosphorylation causes loss of cadherin-catenin complex function, inhibiting cell differentiation and promoting invasiveness (61). On the other hand, AJ components such as β-catenin and p120-catenin are direct substrates of SFK, being phosphorylated in a Src-dependent manner. Phosphorylation of these proteins can result in E-cadherin downregulation and/or loss of the linkage between cadherins and the actin cytoskeleton. This loss can promote the disruption of cell-cell adhesion and contribute to cell migration and invasiveness (12) (62).

Several studies demonstrate that elevated SFK activity is related with clinical parameters. Tumours expressing progesterone receptor displayed higher c-Src kinase activity (63). In a study with 72 samples of breast cancer, all tumours displayed elevated tyrosine kinase activity comparing with normal tissues, and 70% of that activity could be due to c-Src (64). Other study demonstrated that c-Src protein expression and kinase

activity were elevated in breast cancer tissue comparing to normal breast, and c-Src protein levels were also elevated comparing to normal non-cancerous tissue (65).

2.3. Src as a therapeutic target

Assumed the role of SFKs in growth, proliferation, invasion, angiogenesis and metastasis, it is clear the importance of targeting these kinases in order to inhibit their function. Blocking Src activation may slow disease progression and play an important role in adjuvant setting to prevent recurrence and metastasis from residual disease. This inhibition can also reduce the development of bone metastasis and the associated pain (66).

SFKs are activated downstream of receptor tyrosine kinases through displacement of the tail phosphotyrosine from the SH2 domain or via tyrosine phosphatase-dependent dephosphorylation of the regulatory tyrosine. However, those mechanisms are not mutually exclusive, and may both lead to SFK activation (53).

SFKs can also cooperate with tyrosine kinase to mediate important signalling cascades in diverse biological processes, such as in tumour development. Namely, it can control cell proliferation and survival. Src can directly bind to EGFR and phosphorylate the Y845 residue, resulting in increased MEK and MAPK activity and enhanced cell mitogenesis and transformation (54). Src, Fyn and Yes can be activated by PDGFR through its two autophosphorylated tyrosine sites (Tyr579 and Tyr581) in the juxtamembrane region of PDGFR. Mutations of these two sites can repress PDGF-induced Src activation and lead to a loss of binding ability of Src to the receptor. Moreover, coexpression of EGFR and Src can lead to cell hyper proliferation and enhances the tumour migratory and invasion behaviour, namely in breast cancer cells (67).

Concerning angiogenesis, it is frequently activated in cancer, being antiangiogenic drugs approved for treatment of several solid tumours. This process is regulated by multiple cytokines that trigger a cellular cascade favouring endothelial cell migration and proliferation. Src activation is associated with increased expression of proangiogenic cytokines, like VEGF and interleukin 8 (IL-8) (68). Inhibiting Src will block IL-8-mediated VEGFR2 activation, decreasing vascular permeability (69). Besides that, SFKs are involved in endothelial cell function; through the inhibition of Src, Fyn and Yes, it is possible to decrease VEGF-induced endothelial cell migration (70).

2.4. Src inhibitors

Mutations in c-Src are not the main mechanism of SFK activation in human cancers; consequently, inhibiting a single target of Src is improbable to be successful. Concerning selectivity, cellular potency and possible therapeutic application, Src kinase inhibitors have appeared as the most successful therapeutic agents to date. Numerous classes of low-molecular-weight compounds that are ATP-competitive inhibitors of Src-mediated tyrosine phosphorylation have been described (71, 72). Some of these inhibitors even achieve a moderate to high selectivity within the Src family (73), being important because avoid possible interference with immune responses, in case of Lck, Lyn, Hck, Fgr and Blk (74), and proliferation in general, in case of Src, Fyn and Yes (75).

Dasatinib (BMS-354825, Sprycel®; Bristol Myers Squibb) is a highly potent, ATP-competitive kinase inhibitor with antiproliferative activity. Initially, it was developed as a BCR-ABL kinase inhibitor, which is the responsible for the presence of the Philadelphia chromosome in chronic myeloid leukemia (CML). Dasatinib is currently used as second line treatment in this disease, for imatinib-resistant or -intolerant CML and Philadelphia chromosome-positive acute lymphoblastic leukemia (Ph+ ALL) (76). Besides that, other functions were attributed to Dasatinib, being able to inhibit SFKs, but it also inhibits, EphA2, platelet derived growth factor receptor (PDGFR) and c-KIT. Beyond SFKs, it also binds to other tyrosine kinases such as the mitogen-activated protein kinases (MAPK) (77).

Since Dasatinib has been shown to inhibit Src activity in epithelial cell lines, current clinical trials have been trying to use it in solid tumours treatments. It is not clear which is the mechanism that will be more relevant in clinical applications, because it may have several effects on migration and invasion, as well as inhibiting proliferation (78). The inhibitor potential of Dasatinib against SFKs (IC50=0.5 nmol/L) is greater than against Bcr-Abl (IC=1nmol/L) (77).

Dasatinib inhibits cell growth, invasion and angiogenesis, stimulating apoptosis in EGFR-overexpressing breast cancer cell lines. Basal-like or triple negative breast cancer cell lines were showed to be extremely sensitive to this drug (59, 79). It also inhibits almost completely the Src activation and strikingly attenuates the tyrosine phosphorylation of EGFR at residue 845, phosphorylated by c-Src (59). An important therapeutic strategy to overcome EGFR inhibitor resistance is to disrupt EGFR and c-Src interactions. Previous studies have demonstrated that inhibiting EGFR and SFK has a synergistic effect on growth inhibition in models of triple negative breast cancer (60).

3. Cancer Biomechanics

3.1. AFM

I. Principle

Atomic force microscopy (AFM) is a method for high-resolution imaging of any surface including those of living and fixed cells. This technique is used for the characterization of mechanical, electrical and magnetic characteristics of samples to be studied qualitatively and quantitatively (80). AFM process is based on detection of repulsive and/or attractive surface forces (81). A sharp probe (tip) is located at the end of a flexible cantilever which scans over the sample surface in a series of horizontal sweeps (82). An optical detector (photodiode) detects deflections of the cantilever caused by the probe-sample interaction (83). The variation of the point of incidence of the reflected beam on the photodiode measures any minimal bending or twisting of the cantilever, namely, the interaction of the tip with the sample. Forces detected by this mechanism sorts between 10^{-7} and 10^{-12} N (84). Movement of both sample and probe can be scanned by AFM. The sample is gathered on a piezoelectric support (piezo scanner) that also allows the scanning through the displacement of the sample on the *xy* plan, which is responsible for the movement on the *z* axis. When the tip reaches a rise or depression on the sample, there is an alteration in the interaction force. Using piezoelectric scanner, results can be obtained in subnanometer accuracy at relative high speeds (>100 μm/second) and with a spatial resolution that approaches 2 nm (85).

Regarding a feedback mechanism, this change leads to an approach or removal of the sample relatively to the tip. Due to this, the scanning is usually carried out keeping an approximately constant distance between the probe and the sample, which will allow to associate a *z* value to a *xy* pair. These values obtained will be used for the reconstitution of a pseudo-three-dimensional image of the sample (84).

AFM can operate in air, high vacuum and on liquids. Imaging in liquids has the advantage of eliminating the strong capillary forces occurring between probe and sample comparing when performed in air; moreover, it permits the observation of biomolecules under physiological conditions of the living samples. Force applied when working with cells in liquid has to be controlled. Very high force values may cause irreversible damage in the sample and compromise the results (86).

Several modes of approach to this technique have been used, including contact mode, tapping mode and magnetically activated oscillating mode. Regarding contact

mode, it has the advantage of significantly reduce the frictional and other forces to a negligible amount, while the applied force has to be controlled in an exact manner. Damping interactions between the biological molecules and the AFM probe electrostatically can do this reduction (82, 87). In contact mode, the electrostatic double layer repulsion compensates most of the applied force, distributing it over a large surface area of the sample. After correct adjustments of the imaging buffer (pH and ionic strengh), the effective force that still interact locally on molecular structures is appropriately small to hinder the disturbance of the structure of biological macromolecules to can be done imaging at an ideal resolution (82). Besides that, this mode has the disadvantage that the probe loose contact with the sample, sweeping away corrugated when the objects are weakly immobilized (87). Tapping mode and magnetically activated oscillating mode appeared after reducing the frictional forces produced while the tip moves across the sample. These two modes are commonly used and in both cases the AFM cantilever oscillates vertically while performing the objects scan. After correctly adjust the image parameters, the probe touches the sample in a very briefly way at the end of its descending movement (88). These methods are principally used to image single biomolecules weakly immobilized due to the reduction of frictional forces; however, they show lower spatial resolution that contact mode (89, 90).

Imaging is not the only advantage to get from AFM. AFM-based force spectroscopy can be used to quantify properties and interactions of biological systems, in scales of cells to single-molecules, analysing cell mechanics and adhesion (91). Force spectroscopy allows the measurement of intra and intermolecular forces necessary to separate the tip from the sample (92). In this type of measurement, the cantilever moves vertically toward the surface and than in the opposite direction. Through these movements, the vertical displacement of the piezoscanner can be recorded by the cantilever deflection. Resulting in a curve of cantilever deflection against scanner displacement curve, next converted in a force-distance curve, applying for that the Hook's law of elasticity:

$F = -k \Delta\chi$,

where F is the force, k the spring constant of the cantilever and $\Delta\chi$ the length of the deflection of the cantilever (92, 93).

Force-distance curves are composed by two different curves: the approach curve, done when the cantilever enters in contact with sample, and the retraction curve, obtained when cantilever is moved away of the sample (Figure 4). Contact curve is characterized by a small deflection of the cantilever just before the contact point, composed by van der Waals interactions (94). On the other way, retraction curves show differences if they are measured in air or in liquid, but their principle is based on development of a capillary

bridge between the tip and the sample, and it is there when differences appear. In air, as the cantilever approaches the surface, the initial forces are too small to achieve a deflection; at determine moment, the attractive force exceed the value of the spring constant, deflecting the tip and put in contact with the surface. After established the contact point, both the deflection of the cantilever and the repulsive contact force increases; the tip begins to retract from the sample and it often remains in contact with the surface. The liquid curves follow the same principle as the air curves, being the difference at the approach curve that has a different curvature. This difference presents a gradual increase in strength being difficult to establish the point where the tip and sample get into contact; and when the tip is removed from the surface there is a delay in the response of the system due to the effect of the elasticity of the sample. These dissimilarities can lead to a different force curves responses (95).

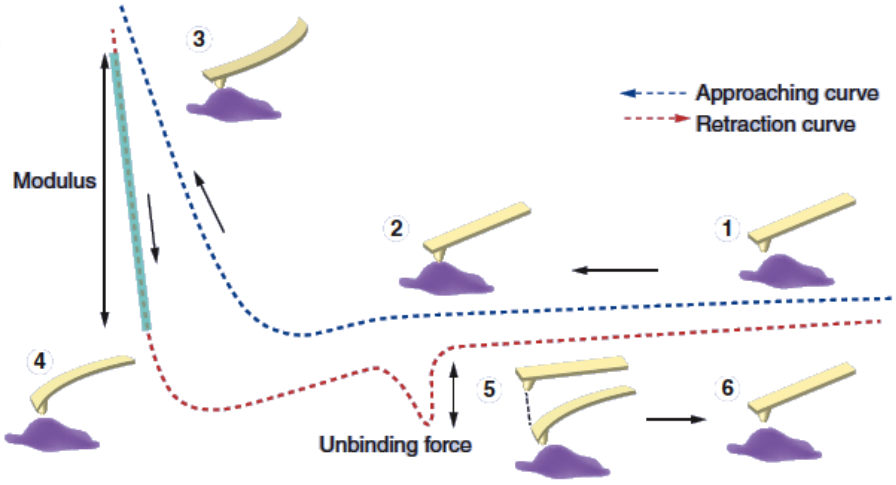

Figure 3 - Typical force curve and cantilever behaviour on living cells. 1, the cantilever with the tip is approaching the sample; 2, the tip contacts with the sample; 3, tip indents into the sample with a specific applied force, 4 tip is moving toward sample, in retract curve; 5, if the tip of the cantilever adhere to the subtract sample, the bends to the sample and after a specific tip-sample distance the bond brakes with a specific unbinding force; and 6, the cantilever achieved again the starting point (zero-deflection position). Adapted from Shi X, 2012 (94).

In air, adhesion force depends of the interaction energies between the tip and the sample; in liquid, besides that interaction, adhesion also depends on the solution. Generally, working with biomolecules, a polymer is formed and connects the tip and the surface of the sample; thus it is generally obtained a negative deflection of the tip and the extension of this polymer will determine the deflection obtained. The extension of the

polymer will stop when the bonds break or the polymer detaches from the tip or surface; after that, cantilever returns to zero-deflection position (92, 96). Force-curves need to be quantitatively analysed by applying polynomial functions. For those are specific requirements to do, as the calibration of the cantilever used in the experiment calculating their spring constant. Cantilever stiffness will depend of the shape and of the properties of the material of fabrication. General values of cantilevers stiffness are between 10-105 pN/nm, however, for commercial cantilevers, a specific spring constant is given (92). There are some calibration methods but the most commonly used is the thermal noise method (97). This method can be used in both air and liquid and it is very simply to apply, giving precision measurements between 10% and 20%.

II. Measuring mechanical properties

Dynamic mechanical properties have been described as intimately linked with physiological functions of living cells. Concerning that, it is possible to quantitatively measure changes in cellular elasticity as a function of time and physiological state, as well as changes in cell adhesion capacities, as cell surface interactions (91). In cancer, nanomechanical analysis is becoming extremely important, mainly regarding the differences in stiffness between normal and malignant cells, being this related with their metastatic potential (96).

Regarding force spectroscopy, there are uncountable applications to be used in this context. Nanoindentation is used to determine elastic properties, like the elastic modulus for biological samples, when the tip indents the cell (97). Hertz model is the most common model used to do the analysis of indentation and to extend to match the experimental conditions concerning the indenters' shape or the thickness of the sample (96). Thus, the Hertzian theory behind this model uses the depth of indentation to assess elasticity, which results in Young's elastic modulus. Specifically, this method allows characterizing the elasticity of biological structures, comparing different types of cells or even organelles (98). The Hertz model approximates the sample as an isotropic and linear elastic solid, also assuming that the indenter is not deformable and that there are no additional forces of interaction between the two parts. Knowing these conditions, the Young's modulus can be calculated. Using AFM to measure cell mechanical properties for cancer diagnosis has some challenges, namely factors that are variable, such as tip geometry, indentation depth and loading frequencies, can lead to a not standardized measurement. Using Young's modulus for diagnosis can also leads to a variance in patient's samples, assuming a flat surface with infinite thickness, which can be different from sample to sample (99).

Initially, AFM was designed to be an imaging tool, but sooner was modified to operate in force scan mode. As a high sensitive microscope, it allows measuring interactions between two opposing surfaces, in single molecule level and with precision of positioning (100). Using AFM in cell adhesion studies has the advantage of obtaining high specificity and wealth of information, quantifying the complex inter and intramolecular interactions that determine the properties of biological molecules and biomaterials (101). Force scans afford information about the individual bond strengths, as well as about the force and work necessary to separate the entire complex formed (102). Single-cell force spectroscopy is applied to measure binding forces between single molecular interaction partners (103). A living cell is attached to a tipless cantilever, place in contact with other cell or substrate and a contact force is achieved. Then, a cantilever deflection-versus-displacement curve is obtained and converted in force-distance curves. Interactions between receptors and ligands are studied measuring the binding forces between receptors or even ligands that are attached to the cantilever and ligands immobilized in a surface (104). These curves release information about detachment work, maximal detachment force and the force of individual bonds (jumps), as well as the formation and unbinding of membrane tethers (105, 106).

Measuring the work that is required to detach both cells can be used to define the adhesion force of the cell. Area under the retraction force-distance curve calculates this parameter describing the energy dissipated during that force experiment (107). Detachment force represents the maximum strength of the interaction of cells surface and classically ranges from several hundreds of piconewtons to nanonewtons, depending on cell shape and deformation properties. Jumps are a bond property that occurs at close distance to the contact point (up to 6-10 mm) and are characterized by a spring-like extension with linearly increasing force before bonds break. Generally occur from the interactions between polymers at the extracellular surface of the cell membrane (85). Membrane tethers designate the other unbinding events observed on the AFM cell-cell adhesion curves. Membrane tethers are described as cytoskeleton membrane adhesions, which after cell-cell separation are characterized by a plateau persisting for more than 0.25 µm., Tethers are formed when cell adhesion molecules adhere to each other and are detached from the intracellular actin cytoskeleton. In this cases, pulling on cell adhesion molecules results in extruding a lipid-nanotube or membrane tether from the cell membrane. Membrane tension and membrane-cytoskeleton anchoring are the main determinates of this force (106, 108).

Studying cell adhesion, application of a force large enough to break all bonds, responsible for the cell-cell adhesion, does not provide information about component parts of the adhesion system. A combination of specific and non-specific interactions is present

as well as the presence of more than one specific ligand-receptor interaction, disables the determination of the contribution of individual elements to the overall binding.

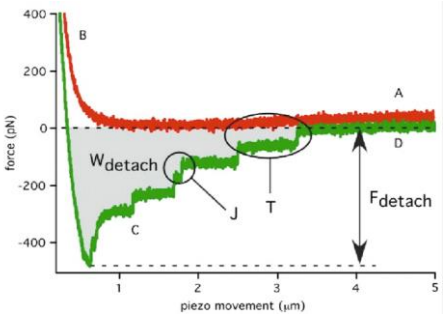

Figure 5 - Schematic example of force curves obtained in cell-cell adhesion measurements with results acquired: work (W_{detach}), detachment force (F_{detach}), jumps (j) and tethers (t).

Regarding the example of the force-curve on Figure 5, there are four regions in these curves. Regions A and B correspond to approach phase, whereas regions C and D to the retraction of the cell on the cantilever from the cell on the substrate. Changes on the retraction from the zero-deflection position represent the adhesion contact between the cell on the cantilever bound to the cell surface. Maximal adhesion force required to separate both cells can be measured from the difference between the baseline and the force minimum point of the largest negative deflection of the cantilever. After this first detach, small events also occur, namely jumps, that correspond to the unbinding of ligand-receptor interactions without a proceeding membrane deformation, and membrane tethers, that correspond to instances where the membrane tether is extruded before the unbinding of the ligand-receptor complex (Figure 6).

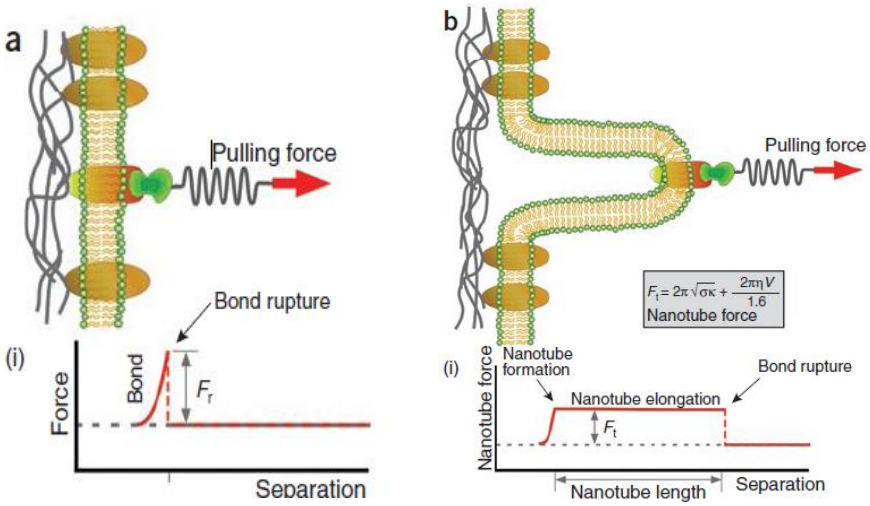

Figure 6 - Schematic examples of detachment forces applied in cells.

a - Cortex-bound adhesion molecule pulled away from the cell surface by the bond ligand. **(i) -** The receptor-ligand bond is mechanically stressed until it ruptures at a force ***Fr,*** event named as jump.

b - Purely membrane bound receptor being pulled from the cell surface at the tip of a membrane nanotube. **(i) -** As depicted, the extension force of nanotubes remains constant at constant extension velocity, and these events are called tethers.

Adapted from Muller DJ, 2009 (107).

3.2. Morphological and mechanical properties of breast cancer cells

I. Role in malignancy and invasion

Tumorigenesis and progression to metastasis are promoted by the disequilibrium in physical and chemical forces that mediate proliferation, differentiation and migration. Structural changes in the extracellular matrix and in the cytoskeleton are, at a molecular level, responsible by tumour initiation and progression (109). During disease, it is known that cells change their physical properties. Atomic force microscopy has been recently used to study changes in cancer cells, by characterizing and quantifying their properties during cancer progression (110). In a study that isolates single cancer cells from patients, the authors observed that they were significantly softer than their normal counterparts (111).

The first study that compared elasticity from normal with cancer cells was done in 1999 and human epithelial bladder cells lines were used (99). Results showed that cancerous cells present a lowest Young's modulus, or highest elasticity, than normal ones. It is known that to efficiently migrate and metastasize, cancer cells need to be fitted in the environment. Studies demonstrate that different substrates can induce alterations in cell elasticity, obtaining different values of Young's modulus, proving a perception of cell's environment, with different actuating capacities (99).

Using breast cancer biopsies of mouse models, investigators found differences between elastic characteristics of normal and malignant cells (112). According to some authors, during early stages of disease, normal cells surround malignant cells, and mechanical interactions of both types of cells may be responsible for extrusion and invasion of unpleasant cells (97). Furthermore, the reorganization of the cytoskeleton has become a specific point of interest regarding changes in cell morphology, motility, adhesion and invasion (113). Changes in the physical properties of tissue cells, especially cell elasticity, have been accepted as an indication of disease, functioning as a marker for cellular phenotypic events associated with cell adhesion and cytoskeletal organization (114). In other study cancer cell stiffness was analysed and the authors observed that a decrease in cell stiffness correlates with an increase in the metastatic potential, being the metastatic cancer cells more than 70% lower than the respective control cells (112). Three-dimensional cell cultures and mouse mammary glands were used to study breast cancer cells in tumour progression. In these models, cancer cells were classified as more rigid than the surrounding tissues, due to a relative stiffening of the peripheral tumour

stroma, being supported by the hypothesis of increasing cellmatrix deposition and crosslinking (115). However, after applying biophysical techniques, the conclusion was that single cancer cells are softer than healthy cells (112).

During invasion processes, cancer cells can aggregate to other cancer cells, and the force of this interaction can be measured through cell-cell interactions (116). Stability of adhesion molecules and integrity of cellular architecture can also be measured during progression events. Nanomechanical properties of tumour cells are associated to their condition, enabling them to change their elastic properties in favour of crossing the cell's barriers, metastasizing the organism, leaving the original site, passing to circulation, adhering in the secondary site and migrating again (117).

II. Evaluating the anticancer activity of a drug

Early diagnosis of cancer, the leading cause of death worldwide, is of particular importance in current medical practice. In recent years, it has been demonstrated that cancer progression is accompanied by alterations in cell mechanical properties. Examination of the effects of an anticancer drug on a cell by atomic force microscopy can be done by three classical measurements: cell imaging and elasticity and cell-cell adhesion (117).

Imaging cell surface after treatments with different drugs provides access to how each drug affects the cell and can help to improve it. In a study using human breast cancer cell (MCF-7), investigators measured the changes in cell's morphological properties, before and after treatment with an anticancer drug, alterporriol L. Using AFM, they concluded that after drug treatment cells became rounded and a decrease of membrane protrusions was observed. Further, the morphological changes observed as blebbing, pores and apoptotic bodies appeared over the cell surface, which are compatible with apoptosis or necrosis (118).

Elasticity can be also classified as a good parameter to evaluate the efficiency of a specific therapeutic molecule. However, depending on the effect that this molecule has on the cell, the results can be opposite regarding Young's modulus. A decrease in Young's modulus can be observed when a specific drug has an apoptotic effect, or a decrease in value of this parameter can represent resistance of tumour cells to a specific apoptotic agent (119, 120).

Cell-cell interactions can also be modified after treatment with specific drugs. These changes could be quantitatively measured using AFM cell adhesion experiments. (116). With the AFM, interaction forces can be determined quantitatively at a single cell level. This approach concentrates on forces arising during the initial cellular contact, as

the cell was not allowed to develop the cell contact for more than 0.1 seconds before cantilever retraction.

RATIONAL AND AIMS

Despite the correlation between mechanical properties of cancer cells and their role in invasion in malignancy, the effect mediated by P-cadherin expression in breast cancer cell's biomechanical properties has never been explored. We believe that P-cadherin aberrant expression, in an E-cadherin wild-type context, may induce alterations in breast cancer cell's morphology and biomechanical properties, being able to explain the migratory and invasive phenotype of these cells. We also hope to find alternative ways to inhibit P-cadherin effect on breast cancer cells.

In order to achieve this, the following specific topics were addressed:

Specific aims:

1. Characterization of the morphological and mechanical properties of breast cancer cells with P-cadherin overexpression.
2. Role of P-cadherin expression in the Src Kinase pathway activation.
3. Impact of Src Kinase inhibition in P-cadherin overexpressing cells.
4. Characterization of the morphological and mechanical properties of P-cadherin overexpressing cells after Src Kinase inhibition.

MATERIALS AND METHODS

Cell culture

Human cancer cell lines were obtained as described: MCF-7/AZ (kindly given by Prof. Marc Marcel, Ghent University, Belgium) and BT-20 from ATCC (American Type Culture Collection, Manassas, VA, USA). Cell lines were routinely maintained at 37ºC, 5% CO_2, in the following media (Invitrogen Ltd, Paisley, UK): DMEM (BT20) and 1:1 DMEM/HamF12 (MCF-7/AZ), both supplemented with 10% heat inactivated fetal bovine serum (Greiner bio-one, Wemmel, Belgium), 100 IU/ml de penicillin and 100 µg/ml streptomycin (Invitrogen). The MCF-7/AZ cell line is a variant of the human breast cancer cell line MCF-7, which expresses basal levels of P-cadherin. MCF-7/AZ cell line was retrovirally stable transduced to encode only EGFP (LZRS-IRES-EGFP plasmid, MCF-7/AZ.Mock cell line) or both P-cadherin cDNA and EGFP (LZRS-P-cad-IRES-EGFP plasmid, MCF-7/AZ.P-cad cell line). MCF-7/AZ.Mock cell line was used as a control.

Antibodies

The following primary anti-human antibodies were used against: P-cadherin (mouse monoclonal IgG1, clone 56, BD Biosciences, Lexington, KY), E-cadherin (rabbit, monoclonal, clone 24E10, Cell Signaling, Danver, MA), p120ctn (mouse monoclonal IgG, clone 98, BD Biosciences), anti-pSrc Tyr 416 (Cell Signalling, Danver, MA), anti-total Src (Cell Signalling, Danver, MA), anti-α-tubulin (monoclonal, clone DM1A, Sigma-Aldrich) and actin (goat polyclonal IgG, I-19, Santa Cruz Biotechnologies, CA). The horseradish peroxidase-conjugated secondary antibodies used were: donkey anti-goat, goat anti-mouse and goat anti-rabbit (Santa Cruz Biotechnologies).

Dasatinib

Dasatinib (BMS-354825, Sprycel®; Bristol Myers Squibb) was used at 100nM. In cell culture was used in proportion of 1:1000 of supplemented medium. DMSO was used as control. Cells were incubated with the drug for 48 hours.

Transfection

BT-20 transfection of validated small interfering RNA (siRNA) specific for P-cadherin (Hs_CDH3_6, GW Validated siRNA, Qiagen, Cambridge, USA) was carried out using Lipofectamine 2000 (Invitrogen Ltd, Paisley, UK) at a final concentration of 50 nM, according to the manufacturer's recommended procedures. After incubation for 5 minutes, the siRNA and Lipofectamine 2000 solutions were mixed, incubated for 20 minutes, and

added to cell culture medium. A negative control, with no homology to any gene, was also used (Qiagen). These cells were incubated with free medium and, after 4 hours, it was replaced by supplemented medium.

Western Blot

Protein lysates were prepared from cultured cells, using catenin lysis buffer [1% (v/v) Triton X-100 and 1% (v/v) NP-40 (Sigma) in deionized PBS] supplemented with 1:7 proteases inhibitors cocktail (Roche Diagnostics GmbH, Germany) and 1:100 phosphatase inhibitor (Sigma-Aldrich, St Louis, MO). Cells were washed twice with PBS and were allowed to lyse in 500 µl of catenin lysis buffer for 10 minutes, at 4°C. Cell lysates were submitted to vortex 3 times and centrifuged at 14000 rpm and 4°C, during 10 minutes. Supernatants were collected and protein concentration was determined using the Bradford assay (BioRad protein quantification system).

Proteins were dissolved in sample buffer [Laemmli with 5% (v/v) 2-β-mercaptoethanol and 5% (v/v) bromophenol blue] and boiled for 10 minutes at 95°C. Samples were separated by an 8% SDS-PAGE, and proteins were transferred into nitrocellulose membranes (Amersham Hybond ECL) at 130 V for 1 hour. For immunostaining, membranes were blocked during 1 hour with 5% (w/v) non-fat dry milk in PBS containing 0.5% (v/v) Tween-20. These were subsequently incubated with primary antibodies, during approximately 1-2 hours or over-night at 4ºC, followed by four 5 minutes washes in PBS/Tween-20 (PBS-T), and incubated with horseradish peroxidase-conjugated secondary antibodies, during 1 hour. Proteins were detected using ECL reagent (Amersham), as a substrate, and blots were exposed to an autoradiographic film.

Atomic Force Microscopy

I. Cell imaging

An atomic force microscope *NanoWizard II* (JPK Instruments, Berlin, Germany) mounted on the top of an Axiovert 200 inverted microscope (Carl Zeiss, Jena, Germany) was used for cell imaging. The AFM head is equipped with a 15-µm z-range linearized piezoelectric scanner and an infrared laser. Cultured cells were washed with phosphate buffered saline (PBS), pH 7.4, and gently fixed with glutaraldehyde solution 2.0 % (v/v) for 10 min at room temperature. Cells were subsequently washed 3 times with PBS and MilliQ water and allowed to air dry at room conditions. The AFM imaging of the cells was performed in tapping mode, in air. Oxidized sharpened silicon tips (ACL tips from Applied Nanostructures, CA) with a tip radius of 6 nm, resonant frequency of about 190 kHz and spring constant of 45 N/m were used for the imaging. Imaging parameters were adjusted to minimize the force applied on the scanning of the topography of the sample. Scanning

speed was optimized to 0.3 Hz, with 512 × 512 acquisition points. Imaging data were analyzed with the JPK image processing v. 4.2.53 (JPK Instruments, Germany). The height, area and volume of each imaged cell were quantified using the SPIP software (Image Metrology, Hørsholm, Denmark) v. 6.2.8. For each experimental condition approximately 10 high resolution AFM images were obtained in two different culture dishes.

II. Cell Elasticity

Nanoindentation experiments were carried out on live cells, at 25°C, in serum free DMEM. For these measurements we used non-functionalized OMCL TR-400-type silicon nitride tips (Olympus, Japan). The softest triangular cantilevers, with a tip radius of 15 nm and a resonant frequency of 11 kHz, were used. The spring constants of the tips were calibrated by the thermal fluctuation method, having a nominal value of 0.02 N/m. For every contact between cell and cantilever, the distance between the cantilever and the cell was adjusted to maintain a maximum applied force of 200 pN before retraction. Cell elasticity was measured on one point of each cell adhered to the tissue culture dish (5 force-distance curves per cell), and on approximately 75 cells at 3 different cell dishes. Data collection for each force-distance cycle was performed at 1.5 Hz and with a Z-displacement range of 4 µm. The force curves were made at the center of the cell, on the top of its nucleus. Data acquired on the nanoindentation experiments (force curves) were analyzed to obtain the cells Young's modulus (E), using JPK Image Processing v. 4.2.53, by the application of the Hertzian model. The probe was modeled as a quadratic pyramid, with a tip angle of 35° (half-angle to face) and a Poisson ration of 0.50. Young's modulus histograms were constructed for each experimental condition studied. The ideal histogram bin size was chosen in order to achieve the best fitted Gaussian model peak length, yielding a selected binning size of 15 Pa. The maximum values of the Gaussian peaks represent different statistical measure of the Young's modulus of the cells. Statistical significance was determined with pair-wise comparisons made with Student's t-test to compare the cells datasets, using a 5% confidence interval. Statistical analysis was carried out using the Graphpad Prism software, v. 5.0.

III. Cell-cell adhesion

Cells were cultured in a tissue culture dish at a low cell density concentration to have only dispersed cells, without reaching cell confluence. On the day of experiment, cells were washed twice with PBS and 1 mL of serum-free DMEM was added. For the cell-cell adhesion experiments, tipless arrow TL1 cantilevers (Nanoworld, Neuchatel, Switzerland) were used, with a nominal spring constant of 0.03 N/m. Cantilevers were cleaned for 15

min with UV light and coated with poly-D-lysine (50 µg/ml) for at least 30 min. Cantilevers were left in the poly-D-lysine solution until used.

Isolated cell suspensions were obtained after 1 h of incubation in PBS (without trypsin treatment) of confluent cells in a separate dish and subsequent pipette dispersion. The cells and the functionalized cantilevers were mounted on the CellHesion module (JPK Instruments, Berlin, Germany), with a 100-µm z-range piezoelectric scanner, connected to the *NanoWizard* II atomic force miscroscope mounted on the top of an Axiovert 200 inverted microscope. 100 µL of cells suspension were injected into the cells substrate dish. Cells were allowed to settle for 30 s before capturing by a functionalized cantilever of one cell using the AFM contact mode. After 30 s of cantilever pressing onto the cell, the cantilever was raised 100 µm on the z-range and the attached cell allowed to rest for 1 min before initiating the contact with an adherent cell on the substrate underneath. Cell-cell contact was established with an applied force of 300 pN, in constant height and closed-loop mode. The AFM tip resonant frequency was maintained at 2 Hz and a cell-cell contact time of 5 s was maintained before cantilever retraction, with a z-range displacement of 50 µm). Five force-distance curves were performed on each cell on the substrate, with a 5 s pause between them. A maximum of 8 different adherent cells on the substrate were tested with the same cell attached to the AFM cantilever.

Statistical analysis

Statistical analyses of the AFM results were performed by Graph Pad Prism version 5.0c software for Mac (Graph Pad Software, San Diego, CA). *p* values less than 0,05 were considered statistically significant. Student's t-tests were used to determine statistically significant differences. Frequency histograms were performed in Origin (OriginLab, Northampton, MA) and Gaussian curves were applied.

RESULTS

1. P-cadherin expression induces alterations in the morphological and mechanical properties of breast cancer cells

We used two already established cell models where P-cadherin expression was manipulated - MCF-7/AZ and BT20. For MCF-7/AZ cell line, P-cadherin cDNA was retrovirally transduced, producing a cell line with P-cadherin overexpression (MCF-7/AZ.Pcad), whereas in BT-20 cell line, which already expresses P-cadherin, its expression was silenced by siRNA. These cell lines were used in these experiments to characterize the morphological and mechanical properties of breast cancer cells with P-cadherin overexpression. On behalf of this, images of living cells were obtained and height, area and volume of the different cell types were measured and compared. Regarding mechanical properties, in order to classify the elasticity of cells, Young's Modulus was measured. Cell-cell experiments were also made with the purpose to obtain values of work, detachment force, jumps and tethers.

1.1. Images

The images obtained from the different cell lines were analysed individually, in order to acquire values of morphological parameters to measure height, area and volume. Histograms with average values, respective standard error of mean and number of cells, for each parameter, were calculated.

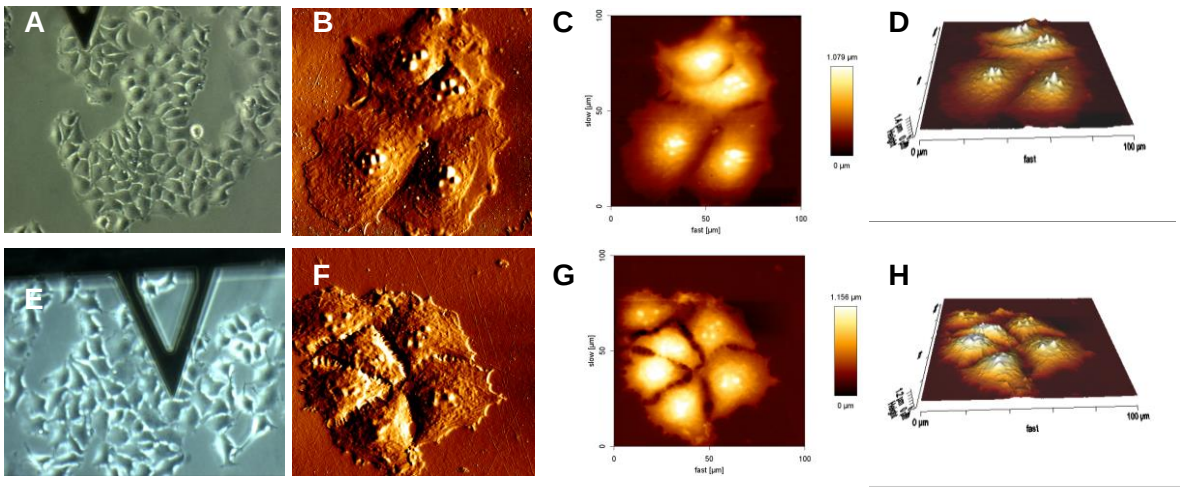

Figure 7 - A-D. MCF-7/AZ.Mock. **A** - Optical image (magnification 16x); **B** - Height image; **C** - Error image; **D** - 3D image.

E-H. MCF-7/AZ.Pcad. **A** - Optical image (magnification 16x); **B** - Height image; **C** - Error image; **D** - 3D image.

P-cadherin overexpression in MCF-7/AZ led to a change in cell morphology, as seen in the images obtained by the AFM (Figure 7). These alterations in cell morphology

were accompanied by an increase in cell area, as well as a significantly decrease height and volume, when compared with control (MCF-7/AZ.Mock). The average height of MCF-7/AZ.Mock was 1203 nm, with a standard error of mean of 20nm. However, MCF-7/AZ.Pcad presented an average height of 1094 nm, having a standard error of mean of 22nm, being significantly lower (p=0.0004) (Figure 8a). The area of control cells was 1.265×10^{9} nm^2 ($\pm6.48\times10^{7}$ nm^2), lower than the area of MCF-7/AZ.Pcad, that was 1.378×10^{9} nm^2 ($\pm7.34\times10^{7}$ nm^2) (Figure 8b). Regarding the volume, the cells with P-cadherin overexpression presented a volume of 2.554×10^{11} nm^3 ($\pm3\times10^{10}$ nm^3) and MCF-7/AZ.Mock cells presented a higher volume, 2.872×10^{11} nm^3, with a standard error of mean of 2.06×10^{10} nm^3 (Figure 8c). The analysis was performed in 56 cells MCF7/AZ.Mock and 63 cells MCF7/AZ.Pcad.

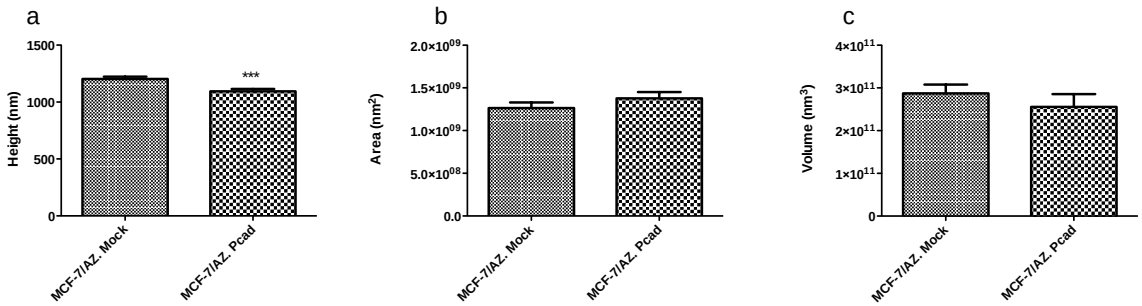

Figure 8 - Histograms representing average height (μm), area (μm^2) and volume (μm^3), with respective standard deviation of mean, comparing MCF-7/AZ.Mock cells and MCF-7/AZ.Pcad.
Significantly differences were observed in height measurement (p=0.0004).

Regarding the other breast cancer cell model, BT20 transfection with P-cadherin siRNA lead to changes in cell morphology (Figure 9). Once again, these alterations were accompanied by a significant reduction of the cell's area, volume and with an increased height. The values of height increased significantly from BT20 siCtr to BT20 siPcad, from 1229 nm to 1498 nm (±39 nm in 43 cells and ±79 nm^2 in 40 cells, respectively) (Figure 10a). The area of BT20 siCtr cells evaluated in 34 cells showed an average of 3.154×10^{9} nm^2 ($\pm1.33\times10^{8}$ nm^2) and decreased to 1.437×10^{9} nm^2 ($\pm1.01\times10^{8}$ nm^2) in 42 BT20 siPcad cells (Figure 10b). The volume of BT20 cells with silencing of P-cadherin also decreased. Cells transfected with siRNA control showed values of 1.346×10^{12} nm^3 ($\pm1.12\times10^{11}$ nm^3 in 43 cells) and with siRNA P-cadherin presented values of 7.376×10^{11} nm^3 ($\pm1.16\times10^{11}$ nm^3 in 42 cells) (Figure 10c).

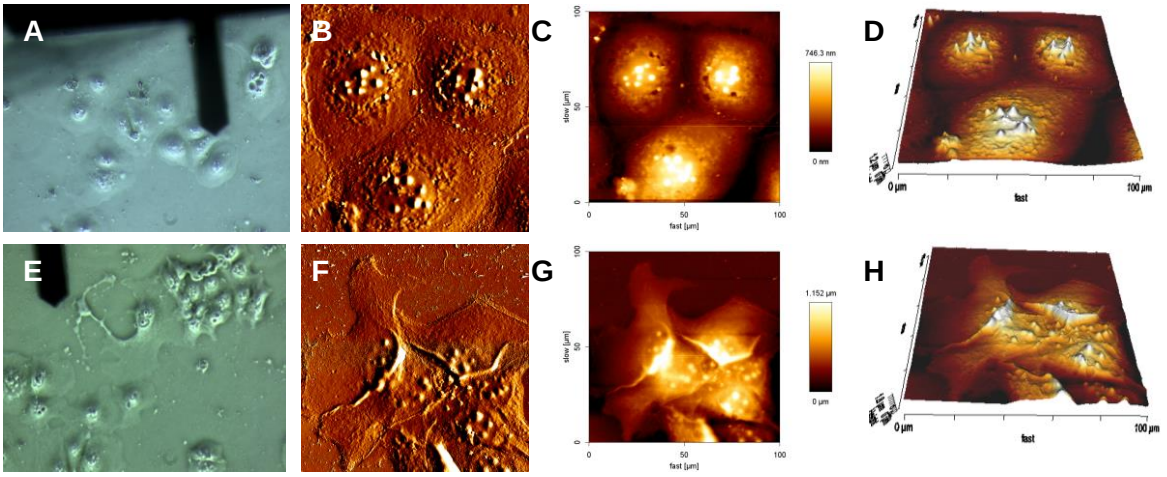

Figure 9 - **A-D**. BT20 siCtr . **A** - Optical image (magnification 16x); **B** - Height image; **C** - Error image; **D** - 3D image.

E-H. BT20 siPcad. **A** - Optical image (magnification 16x); **B** - Height image; **C** - Error image; **D** - 3D image.

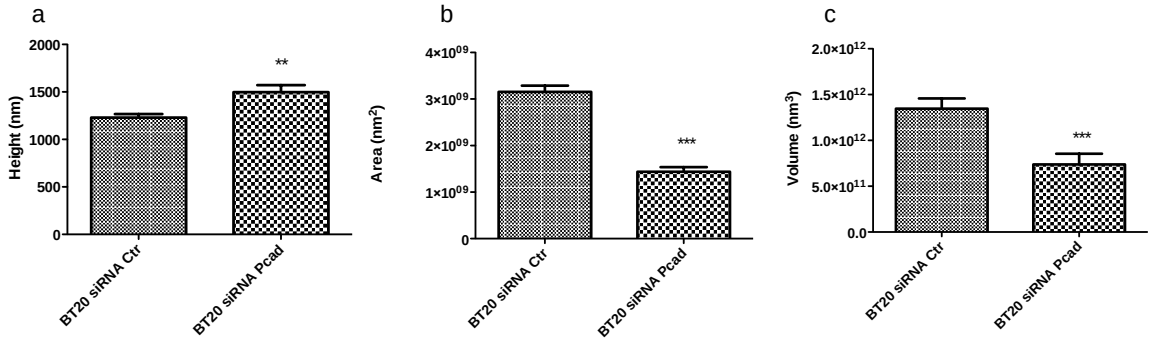

Figure 10 - Histograms representing average height (μm), area (μm^2) and volume (μm^3), with respective standard deviation of mean, comparing BT20 cells silenced with siRNA P-cadherin and control.

1.2. Elasticity (Young's Modulus)

Approaching the surface with the cantilever tip generates a force extension curve. Hertz model is applied to these curves, and results analysed in order to obtain Young's modulus values.

Elasticity was measured according to Young's Modulus. Histogram of frequencies was applied to the values and then a Gaussian curve was obtained for MCF-7/AZ (Figure11A) and BT20 (Figure12A) cell models. Mean values used to compare elasticity were given by the mean value of these Gaussian curves.

MCF-7/AZ.Pcad cells presented a significantly lower Young's modulus values, which indicate higher cell elasticity. In MCF-7/AZ.Mock cells, the mean value of Young's Modulus was 153.1 kPa with a standard error of mean of 0.1044 kPa, measured in 1065

curves. On the other hand, MCF-7/AZ.Pcad cells showed a Young's Modulus value of 117.4 kPa (±0.107 kPa), in 1132 curves analysed. Statistic differences were obtained with a p<0.0001 (Figure 11B).

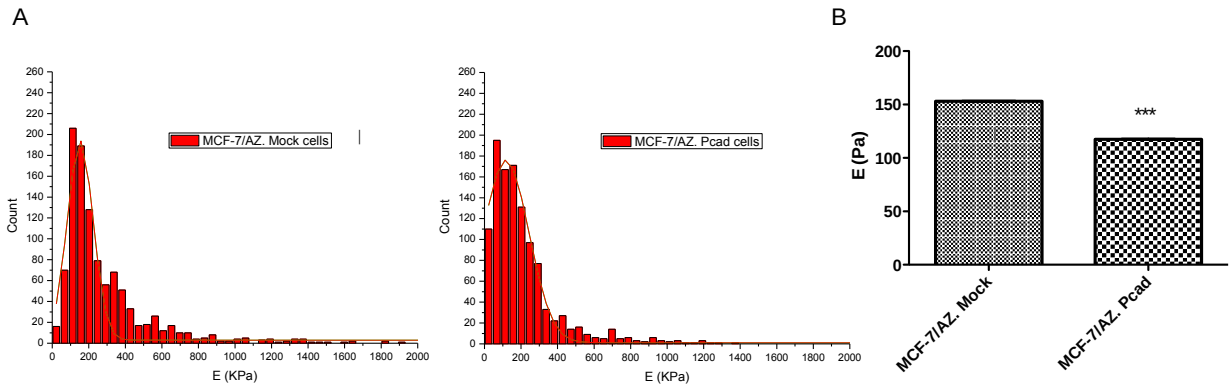

Figure 11 – A) Histograms of Young's modulus values in MCF-7/AZ.Mock and MCF-7/AZ.Pcad and respective Gaussian curve fitted; B) Histogram of average values of Young's modulus in MCF-7/AZ.Mock and MCF-7/AZ.Pcad and respective statistically significance (p<0.0001).

P-cadherin silencing in BT20 induce a significant increase in the Young's Modulus value, revealing a decreased elasticity. BT20 siCtr showed a Young's Modulus of 270.5 kPa (±0.4283 kPa in 1101 curves), whereas the silencing with siPcad increased the Young's Modulus to 300.2 kPa, with a standard error of mean of 0.1871 kPa in 1114 curves (p <0.0001) (Figure 12B).

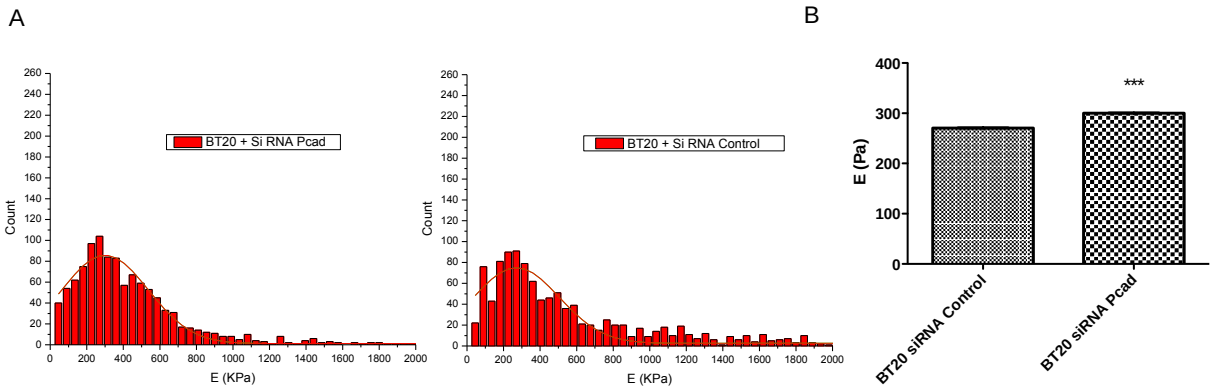

Figure 12 – A) Histograms of Young's modulus values in BT20 siCtr and BT20 siPcad and respective Gaussian curve fitted; B) Histograms of average values of Young's modulus in BT20 siCtr and BT20 siPcad and respective statistically significance (p<0.0001).

1.3. Cell-cell adhesion

Force spectroscopy is capable of determining individual detachments events, likewise the overall force required to detach a cell. Cell-cell adhesion was measured with the purpose of classifying adhesion and detachment of cells in different conditions, either different levels of cadherin's expression, or response to treatments. For each condition, three cells were attached to three different cantilevers, in monolayer eight cells were entered into contact, and from this contact five curves were obtained. From each curve obtained, values of work, detachment force, jumps and tethers were obtained.

1.3.1 Work

The values of work correspond to the area under the retract curve of the cell-cell curves obtained. Cell-cell adhesion for each condition was measured and respective values of work were compared with unpaired t test.

Concerning cell-cell adhesion, we found that the work necessary to separate MCF-7/AZ.P-cad cells was significantly lower than for MCF-7/AZ.Mock cells. The work employed to disaggregated MCF-7/AZ.Mock cells was, in average, 1.254×10^{-15} J ($\pm8.22\times10^{-17}$ J, represented in 84 curves of cell-cell adhesion), and significantly higher than the work necessary to separate MCF-7/AZ.Pcad cells, that was 9.466×10^{-16} J with standard error of mean of 8.687×10^{-17} J, in a total of 121 curves (p=0.0145) (Figure 13A).

Accordingly, P-cadherin silencing in BT20 cells induced increased values of work relative to the respective control. In control cells, the value of work was 6.373×10^{-16} J ($\pm4.941\times10^{-17}$ evaluated in 114 curves). Further, the BT20 siPcad cells presented a value of work of 9.063×10^{-17} J obtained in 113 curves and with standard error of mean of 1.267×10^{-16} J (p=0.0485) (Figure 13B).

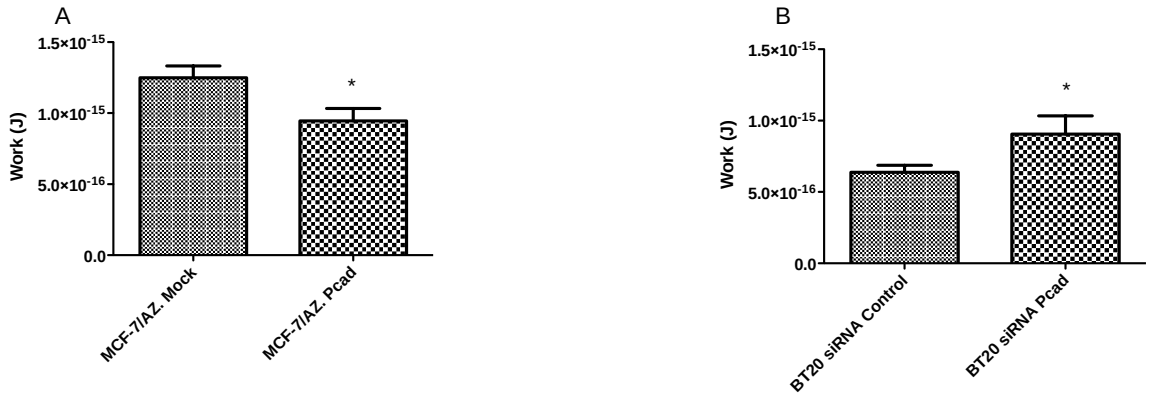

Figure 13 - Histograms of average values of work (J) compared between MCF-7/AZ.Mock and MCF-7/AZ.Pcad, and between BT20 siCtr and BT20 siPcad.
Significantly differences were observed in MCF-7/AZ.Mock vs. MCF-7/AZ.Pcad (p=0.0145) and in BT20 siRNA Control and BT20 siRNA Pcad (p=0.0485).

1.3.2 Detachment force

Detachment forces were measured through the highest peak obtained in the retract curve of cell-cell adhesion curves. Histograms of values were obtained and than Gaussian curves were applied, acquired the mean values and analysed for MCF-7/AZ (Figure 14A) and BT20 cell model (Figure 15A).

Regarding the comparison between MCF-7/AZ.Mock and MCF-7/AZ.Pcad, the second one presented a higher detachment force, with an average value of 153.3 pN (±0.4336 pN) in 110 curves analysed. The control cell presented a value of detachment force of 111.4 pN (±0.5656 pN) in a total of 83 curves observed (p<0.0001) (Figure 14B).

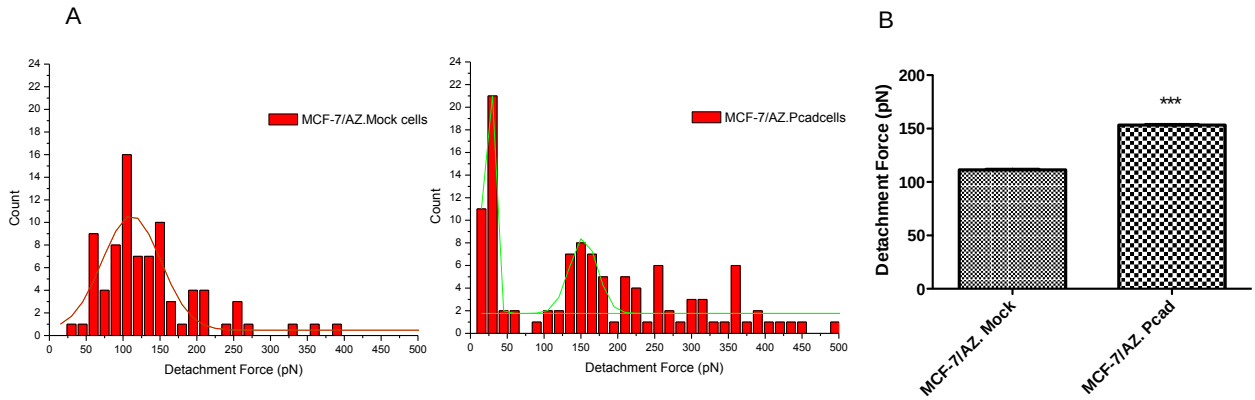

Figure 14 – A) Histograms of Detachment force values in MCF-7/AZ.Mock and MCF-7/AZ.Pcad and respective(s) Gaussian curve(s) fitted; B) Histograms of average values of Detachment force in MCF-7/AZ.Mock and MCF-7/AZ.Pcad and respective statistically significance (p<0.0001).

In BT20 cell line, the ones with silencing of P-cadherin showed a lower value of detachment force when compared with control cells. BT20 siCtr displayed 150.72 pN of detachment force (±7.67 pN) in 117 curves. BT20 transfected with siRNA P-cadherin showed a significantly decreased value of detachment force of 129.14 pN (± 9.5 pN) in a total of 120 force curves (p<0.0001) (Figure 15B).

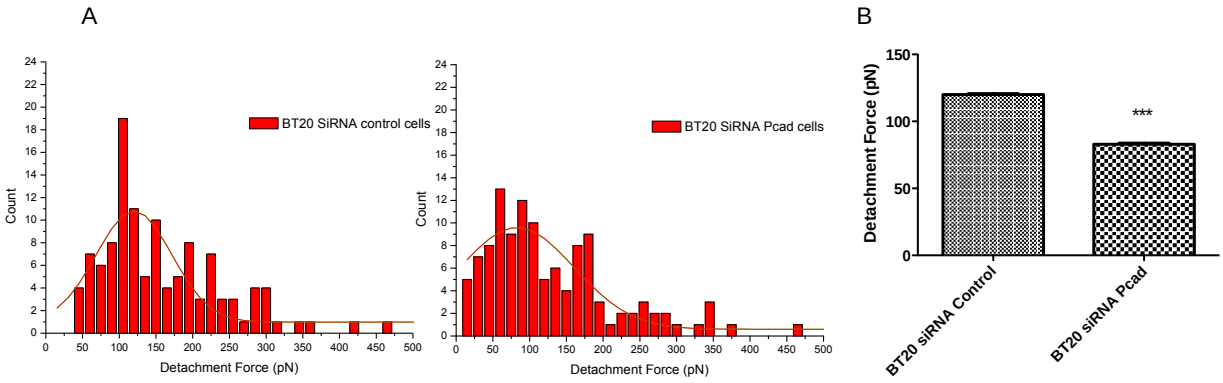

Figure 15 – A) Histograms of Detachment force values in BT20 siCtr and BT20 siPcad and respective Gaussian curve fitted; B) Histograms of average values of Detachment force in BT20 siCtr and Bt20 siPcad and respective statistically significance (p<0.0001).

1.3.3 Jumps

Concerning MCF-7/AZ.Mock, the force measured in jumps to separate these cells was 5.88 pN (± 0.33 pN, in a total of 76 events). The relative events/curve were 0.94. The average value of jumps in MCF-7/AZ.Pcad was 11.06 pN with a standard error of mean of 1 pN in 72 events, being significantly higher (p<0.0001). For each curve, 0.9 jumps were observed (Figure 16A).

In order to detach BT20 siCtr cells, the mean value of jumps obtained was 30.22 pN (±3.16 pN; N=25), whereas in BT20 siPcad cells was 10.91 pN (±0.57 pN; N = 107), being significantly lower for cells silencing with P-cadherin silencing (p<0.0001). The relative events per curve were 0.96 in the first condition and 0.99 in the second one (Figure 16B).

Figure 16 - Histograms of average values of Jumps force in MCF-7/AZ.Mock comparing with MCF-7/AZ.Pcad (p<0.0001) and in BT20 siCtr and Bt20 siPca (p<0.0001)

1.3.4 Tethers

Regarding the cell-cell adhesion curves, values of tethers were also obtained. In MCF-7/AZ.Mock, 395 tethers events were analysed and the value of this force obtained was 6.18 pN with a standard error of mean of 0.15 pN. In MCF-7/AZ.Pcad, the value of tethers was 7.42 pN (±0.65; N=163). The relative events per curve for the control cells were 4.88 whereas for the p-cadherin overexpressed cells were 2.04. Tethers force is significantly higher in MCF-7/AZ.Pcad cells, with p=0.0097 (Figure 17A).

On the other cell line, BT20 siCtr values of tethers were evaluated in 58 events and were 23.26 pN (±2.05 pN). In BT20 siPcad cells, the average value of this force was 10.1 pN, with a standard error of mean of 0.29 pN, evaluated in 692 events. For the control, in each curve were in average 2.23 curves comparing to the silencing P-cadherin cells, that in each curve were present 6.41 events. In these cell lines, the condition that represents the silencing of P-cadherin also showed a significantly decrease in values of tethers (p<0.0001) (Figure 17B).

Figure 47 - Histograms of average values of Tethers force in MCF-7/AZ.Mock comparing with MCF-7/AZ.Pcad (p=0.0097) and histograms of average values of Tethers force in BT20 siCtr and Bt20 siPcad (p<0.0001).

2. Src Kinase signalling activation is increased in P-cadherin overexpressing cells

There are several lines of evidence that tyrosine phosphorylation may play a role in disruption of cell-cell adhesions, due to cadherin phosphorylation and loss of cadherin/catenin association. In breast cancer, the increased activity of c-Src has been associated with tumour initiation, progression and metastasis.

Comparing MCF-7/AZ.Mock with MCF-7/AZ.Pcad, we could evaluate the Src Kinase activation in a cell model with low expression of P-cadherin against overexpression of P-cadherin, respectively. Besides that, Src Kinase signalling activation was also evaluated in BT20 cells, expressing high levels of P-cadherin and BT20 cells without expression of this protein. In order to do that, BT20 cells were transfected with a negative control (siCtr), with no homology to any gene and with siRNA specific for P-cadherin (siPcad).

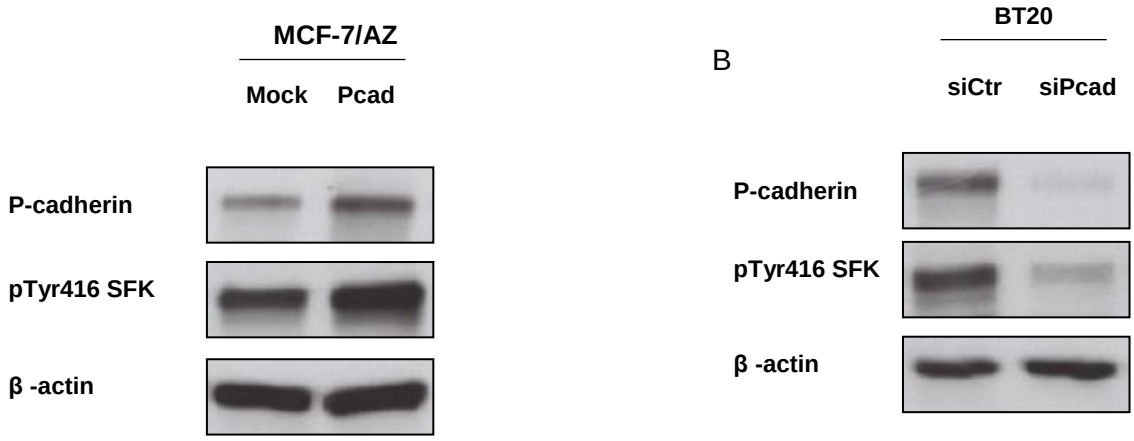

Figure 18 - P-cadherin, pTyr416 and β-actin protein expression in breast cancer cell model with induction of P-cadherin overexpression in MCF-7/AZ cells **(A) or** expression in breast cancer cell model with silencing of P-cadherin overexpression in BT20 cells, using specific small interfering RNA (siRNA) (B)

Observing these results, it was demonstrated that MCF-7/AZ.Pcad cells have a higher expression of P-cadherin, when compared with MCF-7/AZ.Mock cells. There was an increase in the phosphorylation levels of pTyr416 SFK, dependent on the expression of P-cadherin. In MCF-7/AZ.Pcad cells, the expression of pTyr416 SFK was higher (Figure 18A), suggesting that P-cadherin can activate Src signalling pathway.

In parallel, transfection was performed of a P-cadherin overexpressing breast cancer model, BT20, with small interfering RNA for Pcadherin, where we could see that the knock down was efficient, since there was a decrease in P-cadherin expression in BT20 siPcad. Regarding the phosphorylation levels of SFK, there was a clear decrease in the expression of this protein, after silencing P-cadherin in BT20 cells (Figure 18B).

3. P-cadherin induced signalling is repressed by Src Kinase signalling inhibitors

Results shown previously indicated that in P-cadherin overexpressing cells, Src Kinase signalling activation was increased. Besides that, we want to prove that this activation can be repressed using Src kinases signalling inhibitors. For that, Dasatinib was used. To prove its effectiveness in both cell lines, expression of various proteins was evaluated.

In both cell lines, DMSO was used as a control to the treatment with Dasatinib. First we evaluated the effect of Dasatinib treatment in the morphology of breast cancer cells. As observed in the pictures taken with a brightfield microscope (Figure 19), the phenotype of MCF-7/AZ.Pcad and BT20 cells was altered after Dasatinib treatment. Cells treated with SFK inhibitor exhibited a more epithelilal like phenotype, where cells seem to be smaller and more compact than the ones treated with DMSO (Figure 19).

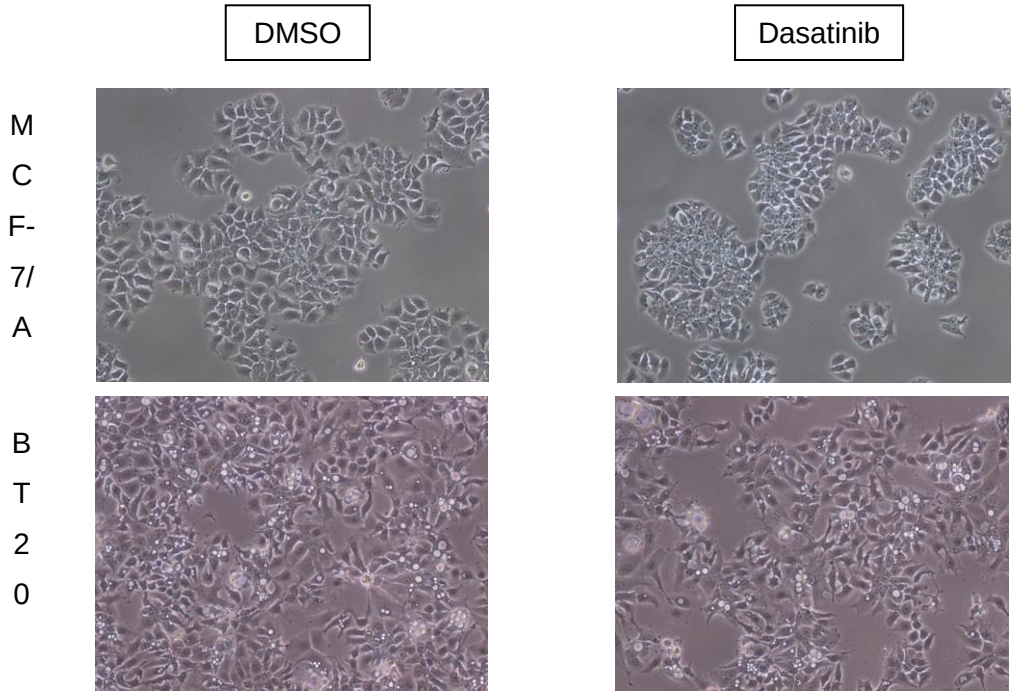

Figure 19 – Optical images from MCF-7/AZ.Pcad and BT20 cells treated with Dasatinib (100nM) and respective control, DMSO.

Further, the expression of P-cadherin, E-cadherin, pTyr416 SFK, total Src, and β-actin (as control of the amount of protein loaded in the gel) was evaluated. E- and P-cadherin expression in both cell models showed no alterations after the treatment with Dasatinib. Regarding Src signalling pathway, Dasatinib treatment of P-cadherin

overexpressing cells lead to a decrease in pTyr416 SFK with no significant alterations in total src levels (Figure 20).

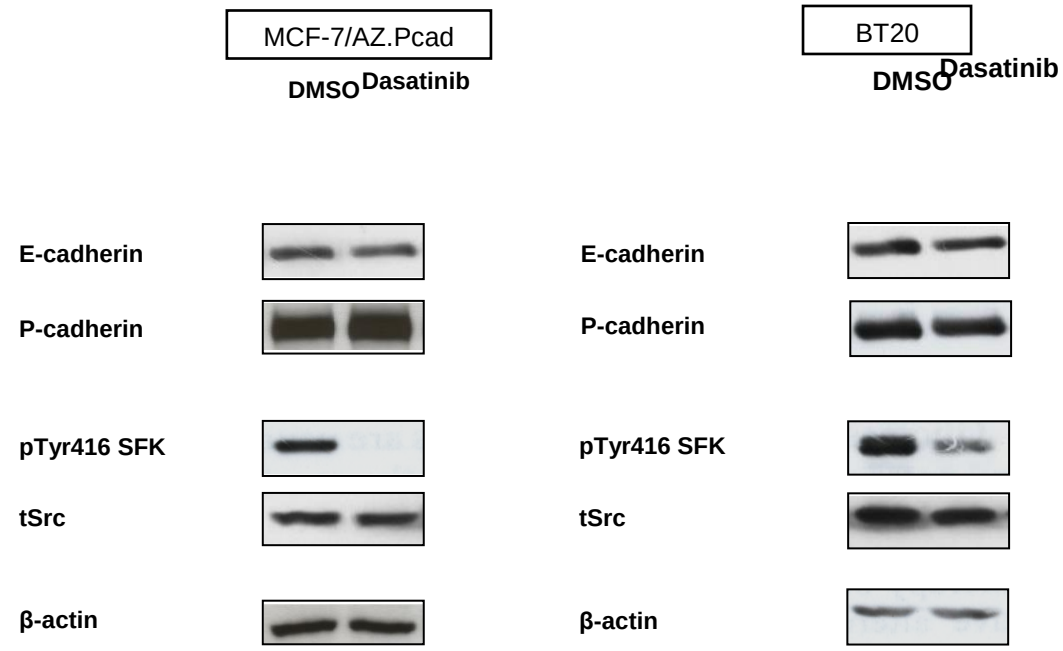

Figure 20 – MCF-7/AZ.Pcad and BT20 cells were treated with Dasatinib. DMSO was used as control. Expression of E-caderin, P-cadherin, pTyr416 SFK, tSrc, and β-actin were evaluated by western blot

4. Src Kinase inhibition with Dasatinib reverts the P-cadherin induced morphological and mechanical properties of breast cancer cells

To characterize the morphological and mechanical properties of P-cadherin overexpressing cells after Src kinase inhibition, cell lines overexpressing P-cadherin were considered, MCF-7/AZ.Pcad and BT20. Results obtained in control cells with DMSO and treated cells with Dasatinib were compared. For measuring morphological properties, AFM images were obtained and values of height, area and volume were analysed. On the other hand, mechanical properties were figured by measuring elasticity of cells, when Young's Modulus was obtained. Cell-cell experiments achieved work, detachment force, jumps and tethers.

4.1. Images

After treatment with Dasatinib, AFM images were obtained and values of morphological properties of MCF-7/AZ.Pcad and BT20 cells were obtained (Figure 21). Height, area and volume were measured in both conditions of the two cell lines. Histograms of respective average values, as well as standard error of mean were obtained, and statistical analysis was performed (Figure 22).

First, analysing the AFM images taken in MCF-7/AZ.Pcad cells after Dasatinib treatment, it was possible to observe a striking change in cells morphology. Src signalling pathway inhibition lead to a more compact cell aggregates, with decreased extension of the cytoplasm (Figure 21).

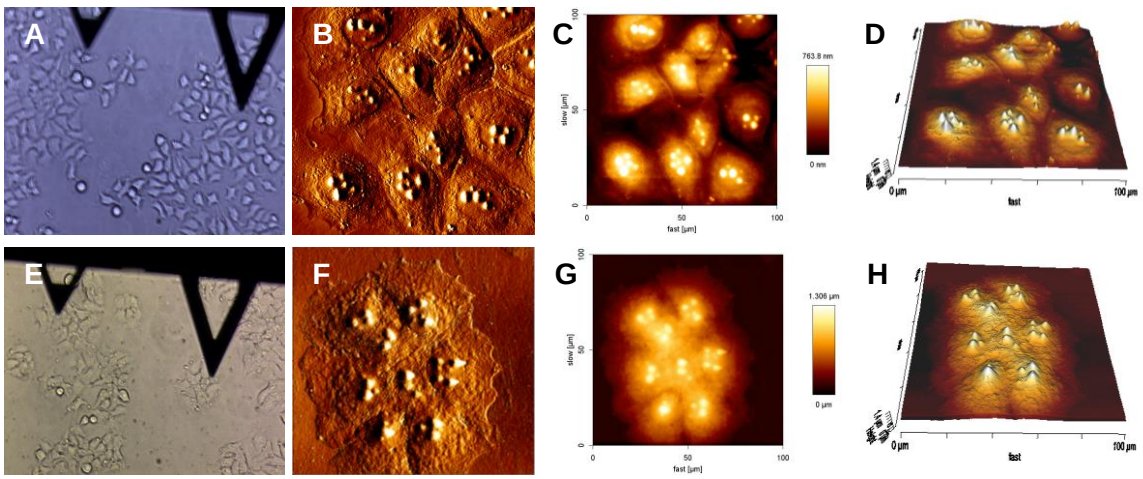

Figure 21 - A-D. MCF-7/AZ.Pcad + DMSO. **A** - Optical image (magnification 16x); **B** - Height image; **C** - Error image; **D** - 3D image.
E-H. MCF-7/AZ.Pcad + Dasatinib. **A** - Optical image (magnification 16x); **B** - Height image; **C** - Error image; **D** - 3D image.

For measuring the height of MCF-7/AZ.Pcad plus DMSO, 139 cells were taken into account. The average height of these cells was 1050 nm (±34.77 nm). In the treated ones, the average height was significantly larger, being of 1232 nm (±52 nm), measured in 139 cells (p=0.0142) (Figure 22A). Regarding area values, the differences obtained were also significant (p<0.0001). MCF-7/AZ.Pcad DMSO showed an average value of area of 8.24×10^{8} nm^2 ($\pm3.94\times10^{7}$ nm^2), according to 79 cells analysed. The value of area was lower in MCF7/AZ. Pcad treated with Dasatinib. In 139 cells taken into account and with a standard error of mean of 2.184×10^{7} nm^2, the mean value was 5.807×10^{8} nm^2 (Figure 22B). Differences obtained in volume results, despite not being significantly, showed a tendency for a decrease in this parameter. In control cells, median volume was 1.78×10^{11} nm^3 ($\pm1.37\times10^{10}$ nm^3) in 79 cells. Treatment with Dasatinib in 139 MCF-7/AZ. cells, reduced the mean volume to 1.517×10^{11} nm^3 ($\pm1.08\times10^{10}$ nm^3) (Figure 22C).

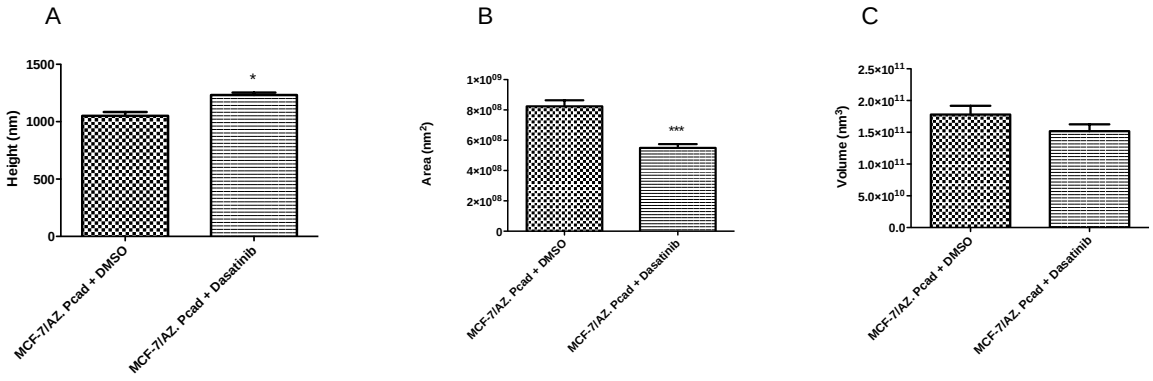

Figure 22 - Representative histograms of average height (μm), area (μm^2) and volume (μm^3), respective standard deviation of mean, comparing MCF-7/AZ.Pcad + DMSO with MCF-7/AZ.Pcad + Dasatinib. Significantly differences were observed in height values (p=0.0142); area - p<0.0001.

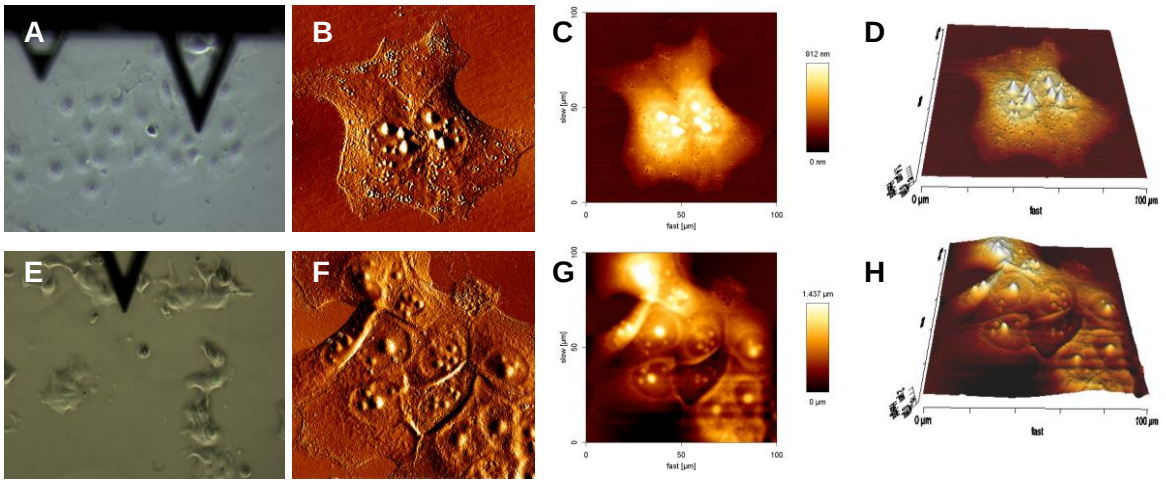

Figure 23 - **A-D**. BT20 + DMSO. **A** - Optical image (magnification 16x); **B** - Height image; **C** - Error image; **D** - 3D image.

E-H. BT20 + Dasatinib. **A** - Optical image (magnification 16x); **B** - Height image; **C** - Error image; **D** - 3D image.

Concerning BT20 cells, treatment with Dasatinib also showed alteration in the phenotype of cancer cells (Figure 23) and significantly increased the height of the cells and reduced area and volume (Figure 24). BT20 plus DMSO cells showed a height of 1227 nm (±36.84) while the treated ones showed 1483 nm (±63.08 nm), being significantly higher (p=0.0105) (Figure 24A). These results were obtained, respectively, in 34 and in 77 cells. Treatment with Dasatinib significantly decreased the area from 2.309×10^{9} nm^2 ($\pm1.32\times10^{8}$ nm^2) in 34 control cells to 9.063×10^{8} nm^2 ($\pm5.51\times10^{7}$ nm^2) in 77 treated cells (p<0.0001) (Figure 24B). Volume was measured in 34 control cells and in 77 Dasatinib treated cells. BT20 DMSO cells showed a volume of 6.897×10^{11} nm^3 ($\pm7.963\times10^{10}$ nm^3), which significantly decreased in BT20 Dasatinib cells (p<0.0001), being of 2.507×10^{11} nm^3 ($\pm1.763\times10^{10}$ nm^3) (Figure 24C).

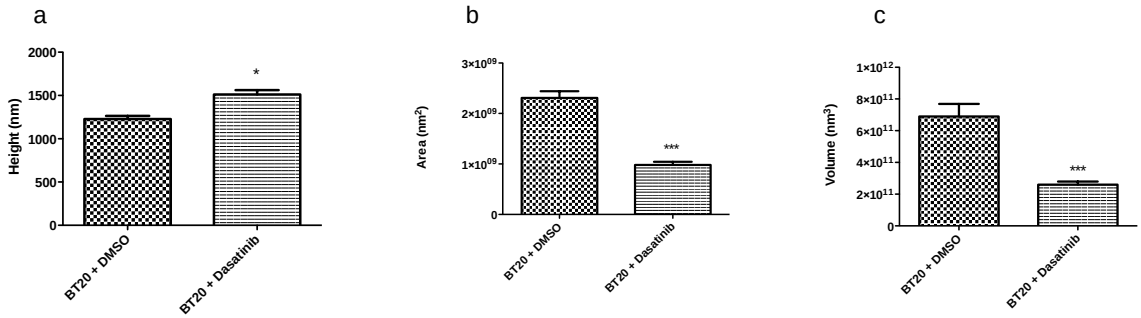

Figure 24 - Representative histograms of average height (μm), area (μm^2) and volume (μm^3), respective standard deviation of mean, comparing BT20 + DMSO with BT20 + Dasatinib.
Significantly differences were observed in height values (p=0.0105) and in area and volume (p<0.0001).

4.2. Elasticity (Young's Modulus)

Indentation was applied to treated cells, force curves were obtained and then analysed in order to achieve Young's modulus values. Frequency histograms were obtained, Gaussian curves fitted and histograms of mean values were acquired (Figure 25A). Statistical analysis was applied, with unpaired t test.

MCF-7/AZ.Pcad cells treated with Dasatinib presented a significantly higher value of Young's Modulus, meaning lower elasticity, comparing with control cells. MCF-7/AZ.Pcad plus DMSO presented a Young's Modulus of 126.3 kPa (±0.043 kPa) obtained in 1132 curves analysed. In 1142 curves of MCF-7/AZ.Pcad cells treated with Dasatinib, the Young's Modulus value was of 132 kPa (±0.046 kPa). This significantly difference was measured with $p<0.0001$ (Figure 25B).

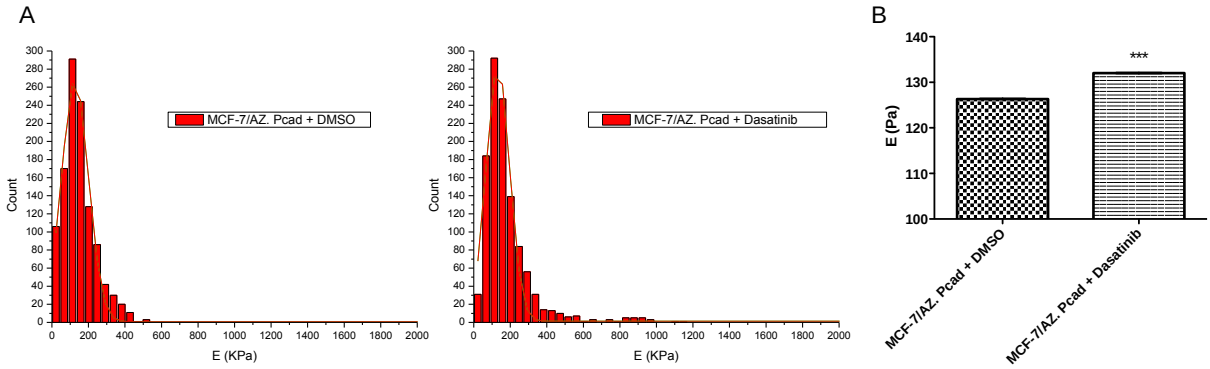

Figure 25 – A) Histograms of Young's modulus values in MCF-7/AZ.Pcad + DMSO and MCF-7/AZ.Pcad + Dasatinib and respective Gaussian curve fitted; B) Histograms of average values of Young's modulus in MCF-7/AZ.Pcad + DMSO and MCF-7/AZ. Pad + Dasatinib and respective statistically significance ($p<0.0001$).

Regarding BT20 cell line, Dasatinib treatment showed the same results, being elasticity significantly reduced in treated cells ($p<0.0001$). BT20 cells with Dasatinib presented a Young's Modulus of 385.3 kPa (±0.3 kPa) whereas the control ones presented 272.9 kPa (±0.25 kPa). The first one was obtained from 1181 curves and the second one of 1108 curves (Figure 26B).

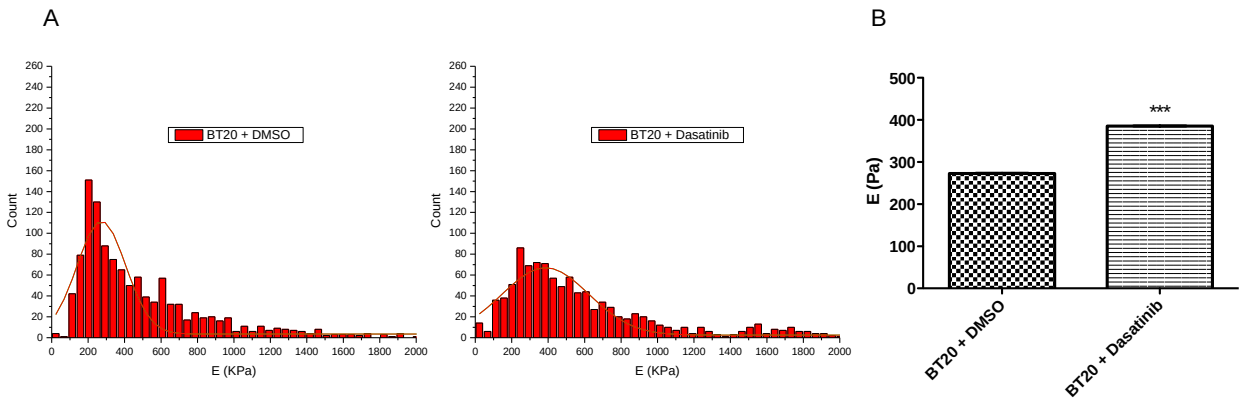

Figure 26 – A) Histograms of Young's modulus values in BT20 + DMSO and BT20 + Dasatinib and respective Gaussian curve fitted; B) Histograms of average values of Young's modulus in MCF-7/AZ.Pcad + DMSO and MCF-7/AZ. Pad + Dasatinib and respective statistically significance (p<0.0001).

4.3. Cell-cell adhesion

4.3.1. Work

According to data obtained through retract curves of cell-cell adhesion, treatment with Dasatinib significantly increased the work in both cell lines. It is necessary to apply more energy to separate treated cells than control cells, in both cell lines.

For MCF-7/AZ.Pcad control cells, the value of work was 1.494×10^{15} J ($\pm1.691\times10^{16}$ J) comparing with cells treated with Dasatinib, which was 2.475×10^{15} J ($\pm1.29\times10^{16}$ J), regarding 73 curves in first condition and 80 in second one (p<0.0001) (Figure 27A).

Considering BT20 cells plus DMSO, the value of work of 8.922×10^{16} J ($\pm8.57\times10^{17}$ J) in 96 curves. On the other hand, Dasatinib treated cells presented 1.348×10^{15} J (1.415×10^{16} J) in 56 curves, being this value significantly higher, meaning that this cells are more difficult to disaggregate (p<0.0001) (Figure 27B).

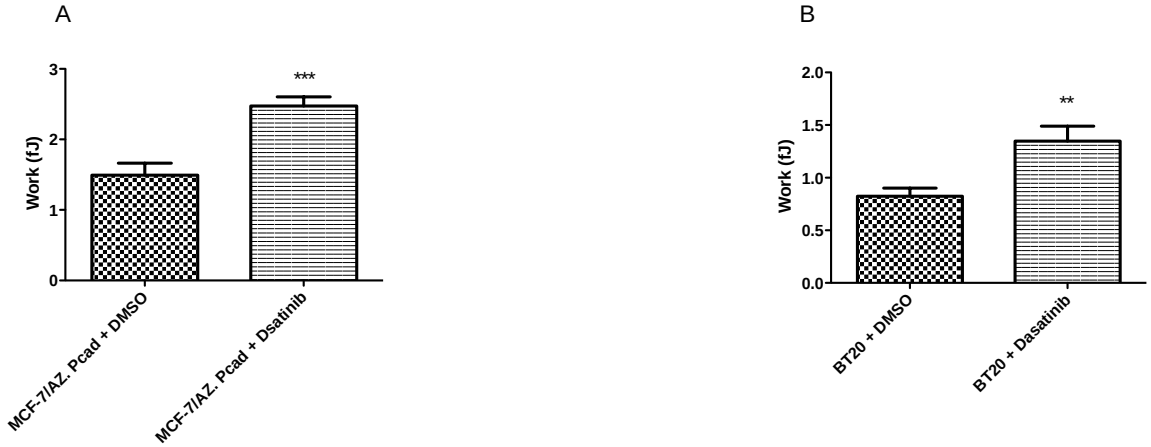

Figure 27 - Histograms of average values of work (J) compared between MCF-7/AZ.Mock and MCF-7/AZ.Pcad (p<0.0001), and between BT20 siCtr and BT20 siPcad (p<0.0001).

4.3.2. Detachment force

Detachment forces were also measured in Dasatinib treated cell models. Values obtained were similar in both cell lines, being both significantly decreased with Dasatinib treatment comparing to control (DMSO treatment).

MCF-7/AZ.Pcad DMSO presented a force of 205.2 pN (±1.6 pN, in 74 curves) and the comparing treated ones, a significantly lower value of 169.4 pN (±1.064 pN, 81 curves, p<0.0001) (Figure 28B).

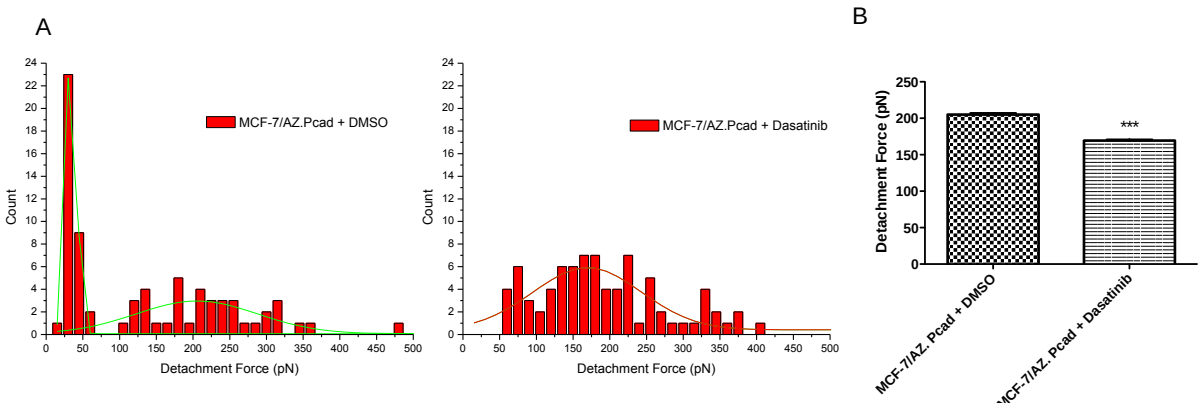

Figure 28 – A) Histograms of Detachment force values in MCF-7/AZ.Pcad + DMSO and MCF-7/AZ.Pcad + Dasatinib and respective Gaussian curve fitted; B) Histograms of average values of Detachment force in MCF-7/AZ.Pcad + DMSO and MCF-7/AZ.Pcad + Dasatinib and respective statistically significance (p<0.0001).

In order to detach BT20 cells, it is needed to apply a force of 120.3 pN (±0.48, in 94 curves). Statistically lower (p<0.0001) is the force needed to disaggregate BT20 cells with Dasatinib treatment; the value of Detachment force was 94.15 pN (±0.48, measured in 56 curves) (Figure 29B).

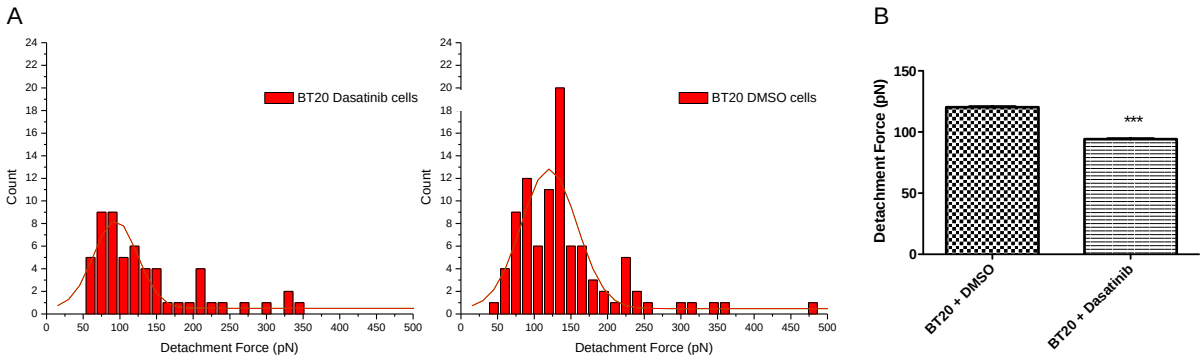

Figure 29 – A) Histograms of Detachment force values in BT20 + DMSO and BT20 + Dasatinib and respective Gaussian curve fitted; B) Histograms of average values of Detachment force values in BT20 + DMSO and BT20 + Dasatinib and respective statistically significance (p<0.0001).

4.3.3. Jumps

Through cell-cell adhesion curves, values of jumps, a specific unbound of membranes, were obtained and analysed. Results obtained for these two different cell lines were similar, having cells with treatment a significantly lower values of jumps and an increase in relative events present in each curve. Thus, in MCF-7/AZ.Pcad DMSO, the value of the jump force was 9.85 pN (±1.29 pN) observed in 40 events. MCF-7/AZ.Pcad Dasatinib cells were analysed and a significantly lower value of 4.93 pN (±0.15pN) was obtained, in 70 events (p<0.0001) (Figure 30A). The relative events per curve were lower in DMSO control, about 0.58 in one curve, when comparing with Dasatinib, with 1.15 events per curve. In BT20 DMSO, jumps force value registered was 29.52 pN (±1.81 pN, in 23 events) comparing to the significantly lower value of 22.18 pN (±1.73 pN, in 16 events) in Dasatinib treated cells (p=0.0078). In the first one, close to 0.79 events were observed in each curve. This value was lower in BT20 plus Dasatinib, being 0.33 events per curve registered (Figure 30B).

Figure 30 - Histograms of average values of Jumps force in MCF-7/AZ.Pcad + DMSO cells comparing with MCF-7/AZ.Pcad + Dasatinib cells (p<0.0001) and in BT20 + DMSO and BT20 + Dasatinib (p=0.0078).

4.3.4. Tethers

The last mechanical property measured in both Dasatinib treated cell lines was tethers, given by cell-cell- adhesion force curves. Tethers increased with treatment in two cell lines, however, only significantly in MCF-7/AZ.Pcad. In DMSO control cells, after analyse 326 tethers events, the value of mean force of 4.2 pN (±0,37 pN) was obtained, comparing with the significantly higher value of 5.34 pN (±0.08 pN) in 401 events of MCF-

7/AZ.Pcad Dasatinib cells (p=0.001). In mean, for each curve, in control condition was registered 4.72 events and in Dasatinib treated 6.57 events (Figure 31A).

Regarding BT20 cells, although no significant differences, results suggest an increase of the mean force of tethers from BT20 DMSO, 29.39 pN (±2.57 pN, observed in 17 events) to BT20 Dasatinib treated cells, 34.08 pN (±1.76 pN), in 73 events. In BT20 plus DMSO, the average number of events in each curve was 0.59 comparing to 1.52 for BT20 Dasatinib cells (Figure 31B).

Figure 31 - Histograms of average values of Tethers force in MCF-7/AZ.Pcad + DMSO cells comparing with MCF-7/AZ.Pcad + Dasatinib cells (*p*=0.001) and in BT20 + DMSO and BT20 + Dasatinib.

DISCUSSION

Cancer initiation and progression can be due to complex molecular and structural changes in the extracellular matrix and cellular architecture of living tissues. However, it remains unclear the responsible mechanism for the majority of these alterations (109). Cancer cells, when compared to normal ones, present tremendous changes in both morphological and mechanical properties. Cell transformation normally initiate with the activation of oncoproteins and/or inactivation of tumour suppressor proteins in a normal cell in an epithelial layer (110). After that, evolution to metastatic cells requires deregulation of numerous cellular processes, like genome stability, proliferation, apoptosis, motility and angiogenesis.

Cell-cell adhesion, namely the one regulated by cadherins, has a crucial role in these processes, since these serve to mechanically couple cells. In response to external forces cells may stiffen, change their shape or alter their behavior including gene expression. These changes involve multiple signaling pathways, and many of the responses ultimately affect the cytoskeleton of the cell.

P-cadherin belongs to the classical cadherin family of proteins and interacts intracellularly with the catenin's family of proteins. Its expression is mostly found in basal–like tumours, which is a subgroup of breast carcinomas of high histological grade and poor patient survival (2) and with no specific target therapy to date. Recently, we described P-cadherin as a breast cancer stem cell marker (3), and we also showed that it has a key role in some acquired cancer hallmarks, since its overexpression in breast cancer cells promotes *in vitro* cell migration and invasion (4,5). We demonstrated that P-cadherin *in vitro* effects are due to inhibition of the E-cadherin suppressive invasive function, by disruption of the E-cadherin/p120-catenin complex at the cell membrane (6).

Although the functional effects of P-cadherin in tumour progression have been explored, nothing has been done to evaluate how its expression affects the morphology and mechanical properties of cancer cells. Recognition of the mechanical properties of cancer cells can help to understand the physical mechanisms responsible for cancer metastasis, beyond other alterations responsible for that process. These alterations in the mechanical properties of cancer cells can be used as biomarkers in early detection of cancer, as well as anti-cancer drug efficacy tests.

Recently, recurring to techniques such as AFM, it is now possible to study the mechanical influences acting on biological structures at molecular levels (99), as well as alterations in morphological properties, that may be altered in diseases conditions or in cells with different molecular characteristics (121).

Considering all that, our aim was to evaluate the effect of P-cadherin expression in the mechanical properties of breast cancer cell lines. For that, we used two established

cell models where P-cadherin expression was manipulated - MCF-7/AZ and BT20. For MCF-7/AZ cell line, P-cadherin cDNA was retrovirally transduced, producing a cell line with P-cadherin overexpression (MCF-7/AZ.Pcad), whereas in BT-20 cell line, which already expresses P-cadherin, its expression was silenced by siRNA. AFM images were obtained, as well as indentation and cell-cell adhesion assays in both models. Then, we obtained two cell lines with lower P-cadherin levels (MCF-7/AZ.Mock and BT20siPcad), and two cell lines with P-cadherin overexpression (MCF-7/AZ.Pcad and BT20siCtr).

Morphological alterations due to the lack of expression or overexpression of P-cadherin could be observed. Expression of P-cadherin, in a wild-type context of E-cadherin expression, leads to a significant decrease in cell's height, proved in both models used. Not so significantly was the variation of values of area that were increased in the cell lines with expression of P-cadherin. Regarding the volume parameter, P-cadherin expression shows contradictory results, depending on the cell model. In MCF-7/AZ cell line, P-cadherin overexpression leads to a tendency to promote a decrease in cell volume, whether in BT20 cell line has the opposite effect, increasing significantly the cell volume. These differences obtained in volume values can be due to slight differences found in the other parameters. The evaluation of volume is obtained by multiplying the values of area and height. By registering small variations in these measures, we can observe a difference in the values of volume, which can lead to different results. However, this data demonstrate that P-cadherin expression, or lack of it, leads to changes in cell morphology, becoming these more flat, which is a characteristic associated with a more migratory and invasive phenotype. These results correlate well with our previous observations concerning P-cadherin's role in breast cancer cell invasion and migration, but also having the knowledge that a tumour cell changes its shape and its internal scaffold (cytoskeleton) when there is tumour progression (122).

The stiffness of cancer cells, compared with normal ones, is often evaluated in order to better understand mechanical properties of these cells. Several studies have demonstrated that cancer cells are significantly softer than their normal counterparts (109), characteristic of the ability of cancer cells to metastasize or spread (122). Regarding AFM measures, indentation of cells can be obtained, as well as values of Young's modulus. In our models, we could observe that P-cadherin expressing cells (MCF-7/AZ.Pcad and BT20 siCtr) showed a decrease in Young's modulus values, representing an increase in elasticity of cells, when compared with MCF-7/AZ.Mock and BT20siPcad, respectively. Once again, these results seem to be in accordance with what has been described concerning cell stiffness and cancer cell invasion. Several studies have shown a reduction in stiffness with increasing metastatic efficiency in human cancer cell lines, using several different *in vitro* biochemical assays (112). A study comparing

elasticity of normal human bladder epithelial cells with cancerous ones demonstrated that normal cells are stiffer than cancer cells, attributing this to the reorganization of the cytoskeleton due to the oncogenic transformation (99). These previous results obtained by other groups, validate our *in vitro* results, since P-cadherin overexpressing breast cancer cells show an aggressive biological behaviour compared with the ones with lower levels of this protein.

Cell-cell adhesion is another parameter that can be altered in cancer. In breast cancer, E- and P-cadherin co-expression affects invasion capacity, stabilization of the cadherin/catenins complex and, consequently, cell-cell adhesion (43). In our study, cell-cell adhesion was measured and values of work, detachment force, jumps and tethers were obtained. Regarding the work parameter, it can be defined as the work needed to disaggregate cells from each other, after a contact has been established. In both cell models, it was showed a significant decrease of work in cells that overexpress P-cadherin. As was known, concomitant expression of E- and P-cadherin leads to a decrease in cell-cell adhesion, what can be responsible for enhancing the migratory and invasiveness capacity of cancer cells. This perturbation in the expression of cadherins leads to an abnormal function of cadherin/catenin complex, which will result in loss of intercellular adhesion and in a possible consequent cell transformation and tumour progression. Besides that, reduced cell-cell adhesion is important both in early and late stages of carcinogenesis and is associated with loss of contact inhibition of proliferation, allowing the escape from growth control signals (123). Considering these results, we can hypothesize that despite MCF-7/AZ.Mock and MCF-7/AZ.Pcad are both cancer cell lines, the second ones presents more invasive mechanical properties, due to their increase in this parameter. In case of BT20 cells, it is acceptable to say that after silencing P-cadherin expression, the cell-cell adhesion increases, which can be responsible for a decreased invasive capacity and aggressive phenotype.

Regarding detachment force results, they were opposite to work results. That is, P-cadherin overexpression led to an increased detachment force. Contrarily of what can be initially supposed, these results are not contradictory. Work values are obtained through the area under the curve, measured in the force-distance curve, while detachment force is measured through the highest peak; so, when we get a superior value of area (work), it is expected that detachment force would be slower, not leading to the presence of a sharp peak (DF). An increase in detachment force indicates a violent cell detach, where the intercellular bonds are quickly broken, without membrane invagination during the process, being applied a minor work. In agreement with this data, detachment force values significantly increased, when we compared MCF-7/AZ.Mock with MCF-7/AZ.Pcad, and significantly decreased, when compared BT20siCtr with BT20siPcad. These results led us

to conclude that in presence of P-cadherin, the detachment is quicker, existing a greater peak in the curve, but a minor area. These results corroborate the hypothesis that aggressive tumour cells present decreased cell-cell adhesion. Previous studies also confirm this data, demonstrating that cell-cell adhesiveness is generally reduced in human cancers. Besides that, loss of cadherin-mediated adhesion may also act by promoting tumour cell detachment from the primary site, resulting in dissemination of malignant cells to distant organs (124).

In force-distance curves, values of jumps and tethers can also been obtained. Once again, results of both cell models showed the same evidences. Expression of P-cadherin led to a significant increase of force of jumps and tethers; silencing P-cadherin in BT20 cells led to a significant decrease of these forces. In this case, the force of small detachment events is significantly higher in cells that overexpress P-cadherin. This can demonstrate that the adhesion forces are weaker and less consistent, what leads to an easier cell detachment.

Number of relative events per curve was also obtained, for each type of force. For jumps force, there were no alterations in different cell conditions, as well in different cell lines. In the four conditions analysed, there was about one event per curve; this would mean that, during the detachment process of these cells, there is a jump recorded. This lack of difference in both conditions eventually reveals that in these cell lines there are few detachment events in a close distance to the contact point of cells, as well as that the differences in P-cadherin expression does not influence this type of bond property. Comparing MCF-7/AZ.Mock with MCF-7/AZ.Pcad, we demonstrated a decrease to near half of the events per cell, while comparing BT20siCtr with BT20siPcad, tethers presence increased almost three times. Regarding literal definition of tethers, we can conclude that the separation between cells was more frequently larger than 100mm in MCF-7/AZ.Mock and BT20 siPcad. Besides that, this increased number of tethers per curve in cells with lower P-cadherin expression indicates that cell adhesion molecules are attached to the intracellular actin cytoskeleton, being more difficult to perform this detach.

Differences in cell-cell adhesion and cell elasticity can be explained by evidences showing that the expression of both cadherins leads to a delocalization of catenins to the cytoplasm, which will originate a disorganization of the actin cytoskeleton. Previous results demonstrate the same evidence, indicating that E- and P-cadherin heterodimers are not efficient in the stabilization of a strong cadherin/catenin complex at the cellular membrane. These cells will show an aberrant cell behaviour, being more aggressive and with increased metastatic capacity (43).

After the analysis of previous results, we can conclude that the presence or absence of expression of P-cadherin has relevance in structuring the cell's cytoskeleton,

being evident in differences obtained in mechanical and morphological properties. Apart from P-cadherin, it is also important to understand which mechanisms downstream of this protein can be important both for growth and tumour progression. In this case, numerous evidences show that tyrosine phosphorylation likely plays a role in the disruption of cell-cell adhesions, phosphorylating cadherin and leading to a dissociation of cadherin/catenin.

Considering that, we aimed to understand if P-cadherin mediated signalling could be through Src Family Kinase pathway activation. Using the same two models, we could observe an increase in the expression of pTyr416 (SFK phosphorylated) in P-cadherin overexpressing cells. This effect was not observed in the total levels of Src, showing that P-cadherin aberrant expression in E-cadherin positive cells, promotes activation of Src signaling pathway. Src has been implicated in the development and progression of several types of cancer and has been the subject of numerous studies. Src kinase is regulated by growth factors, cytokines, cell adhesion and antigen receptor activation, and is involved in controlling several cellular processes, including cell proliferation, migration, invasion and survival.

Once proved the influence of expression of P-cadherin in phosphorylation of SFKs, the effect of these kinase inhibitors was also studied. Therefore, SFKs inhibitors were used to reverse activation of Src and subsequent evaluate its effect on P-cadherin expression, as well as the inherent morphological and mechanically changes of cells properties.

Dasatinib (BMS-354825) was identified as a highly potent inhibitor of Src family kinases and Abl kinases, which shows anti-proliferative, anti-migratory and anti-invasive activity in solid tumors. Interestingly, it is currently in clinical trials for triple-negative breast cancer, in which P-cadherin expressing tumors are included. Taken these observations into account, we decided to treat with Dasatinib the P-cadherin overexpressing cells (MCF-7/AZ.Pcad and BT20 siCtr), which are the ones with SFK signalling activation. Protein expression analyses demonstrated that Dasatinib treatment reduce the expression of pTyr416 in both cell lines, as expected. Besides that, morphological alterations were observed in treated cells. Src inhibition in P-cadherin overexpressing cells led to striking alterations in the cell's phenotype, with decreased cytoplasmic extensions and membrane protrusive structures. However, it was important to understand if these phenotypic and protein expression alterations also interfere with the mechanical and morphological cell properties, confirming the P-cadherin induced Src expression.

In order to do that, AFM studies were also applied in cells with P-cadherin overexpression treated with Dasatinib. To understand the morphological and mechanical alterations caused by Dasatinib in MCF-7/AZ.Pcad and BT20 cells, height, area and

volume were measured through the AFM images obtained; elasticity was obtained through the Young's modulus of the force-distance curves; work, detachment force, jumps and tethers were obtained through the force-distance curves of cell-cell adhesion experiments.

Dasatinib treatment significantly increased the height of both cell lines and decreased the area; volume of cells significantly decreased in BT20, but in MCF-7/AZ.Pcad only showed a tendency. Together, these results suggest that the Dasatinib treatment reverted the more invasive phenotype to an epithelial-like phenotype, with more polarized cells and with a more defined cellular architecture, also present in cells with lower P-cadherin expression values.

In what concerns cell's stiffness, the results of both cell models are concordant. Values of Young's modulus significantly increased with Dasatinib, which means that treated cells showed less elasticity than untreated ones. Observing these results, we hypothesise that this reduction in cell elasticity is linked with the reorganization of cell cytoskeleton, promoted by the absence of Src activity, induced by Dasatinib. This reorganization makes the cells with more height and less elastic, which indicates that they probably have reduced invasive capacity.

Concerning cell-cell adhesion studies, there was a significant increase in values of work in both cell lines treated with Dasatinib and a concomitant decrease of detachment force applied. Once again, these are not opposite results. The increase of work of de-adhesion in treated cells indicate that the link between them is stronger when compared to the untreated ones. This suggests that the inhibition of SFK will make the cells more adherent to each other, with stronger linkage between them and being more difficult to spread. The decrease of detachment force, once again, can be explained by the conformation of distance-force curves. When there is an increase in the area under the curve (work), the maximum point is smaller (detachment force), what can explain these results. Besides that, if cells are more attached to each other, the work necessary to disaggregate them is superior, but the maximum force could be minor, due to a constant pressure that makes a constant force and detach.

More complex are the results obtained with jumps and tethers. Regarding jumps, their force values significantly decreased in both cell lines, while increased in tethers, but only in a significant way in MCF-7/AZ.Pcad cells. This decrease in jumps force in treated cells indicates that the force applied in detach events in a close distance to the contact point is minor when compared to untreated cells; but the increase in tethers force reveals that to separate connections larger than 100 nm, the forces applied need to be higher in treated cells. But the main differences within these results appeared in the relative events per curve. In the case of MCF-7/AZ.Pcad, the relative number of jumps per curve

duplicates from the untreated to treated cells; but in the case of BT20, this number reduces to half, being the only inconsistent result. In case of tethers, in both cell lines, the number of events per curve increased in treated ones; however, in MCF-7/AZ.Pcad cells, the difference was bigger as well as the number of events. These differences obtained in these results may be due to the difference of both cell lines, whereas MCF-7/AZ.Pcad are luminal cells and BT20 are basal-like cells, and not to the Dasatinib treatment.

After verifying these results, we can observe that Dasatinib have effects in protein expression in cell lines that overexpress P-cadherin, reducing the expression of the phosphorylated form of SFK (pTyr416) with no alterations in total Src. AFM results for Dasatinib treatment shows the morphological and mechanical alterations that were concordant with these previous results. This drug turns the cells more polarized, with an epithelial-like phenotype, probably due to the lack of Src activity. The increased rigidity of treated cells also corroborates this fact, since cells with an invasive capacity are less stiff. A study done with Ishikawa cells (derived from well-differentiated human endometrial epithelial adenocarcinomas) shows that with the application of *Paclitaxel* (a mitotic inhibitor used in chemotherapy) there was a decrease in stiffness of these cells after treatment (119). A study developed with human prostate cancer cells, showed that Dasatinib inhibited migration and invasion (125). Besides that, alterations in cell stiffness correlates with metastatic cell potential and cytomechanical measurements with immunohistochemical analysis suggests that nanomechanical measurements of cancer cells has potential for detection of cancer, as well as drug screening (112). On the other hand, several studies show that Dasatinib treatment increases the expression of E-cadherin and stabilize its expression in cell-cell junction, which will inhibit tumour cell migration and invasion (78). This increase of expression of E-cadherin at the cell membrane, due to Dasatinib effect, will increase the cell-cell adhesion capacity, which corroborate our results.

Taken together, our findings demonstrate that overexpression of P-cadherin in breast cancer cells promotes alterations in the biomechanical properties of breast cancer cells, correlating with the increased migratory and invasive potential of these cells. These morphological and mechanical properties may be associated with the activation of the SFK signalling mediated by P-cadherin expression in an E-cadherin wild-type context. In this way, treatment with Src inhibitors, such as Dasatinib, will have an effect on P-cadherin's signalling, inhibiting the biomechanical alterations promoted by P-cadherin expression.

CONCLUSION

Regarding the initial aims of this Master thesis, we believe that we have successfully addressed most of the questions we set out to answer.

The data presented and discussed herein allowed us to conclude that:

1. P-cadherin overexpression promote morphological and biomechanical alterations in breast cancer cells, that can be measured by AFM, turning cells more flat, more elastic and less cohesive.
2. P-cadherin overexpressing cells show an increase in Src Family Kinase pathway activation, demonstrated by p-Tyr416 increased expression.
3. Dasatinib treatment of P-cadherin overexpressing cells promoted the decrease of p-Tyr416 SFK, with no significant alterations on total levels of cadherins or total Src.
4. The treatment with Dasatinib reverted the P-cadherin-induced phenotype and biomechanical properties, allowing cancer cells to adopt a more “epithelial-like” phenotype with an increase in cell stiffness and in cell-cell adhesion.

In conclusion, this study contributed to clarify the role of P-cadherin expression in the biomechanical properties of breast cancer cells. Moreover, it showed how AFM can be an essential tool to study these morphological and mechanical alterations, and how they correlate well with tumour cell’s behaviour. AFM measurements demonstrated that P-cadherin represses the normal cell-cell adhesion mediated by E-cadherin in cancer cells, justifying the increased invasive phenotype, besides the cell-cell adhesion maintenance, but also that Dasatinib treatment can revert the P-cadherin-induced changes.

This work reinforced the importance of P-cadherin expression as a prognostic factor for breast cancer patients, and supports the development of new therapeutics to control aggressive carcinomas co-expressing both epithelial cadherins.

REFERENCES

1. Paredes J, Figueiredo J, Albergaria A, Oliveira P, Carvalho J, Ribeiro AS, et al. Epithelial E- and P-cadherins: role and clinical significance in cancer. Biochimica et biophysica acta. 2012;1826(2):297-311.
2. van Roy F, Berx G. The cell-cell adhesion molecule E-cadherin. Cellular and molecular life sciences : CMLS. 2008;65(23):3756-88.
3. van Roy F. Beyond E-cadherin: roles of other cadherin superfamily members in cancer. Nature reviews Cancer. 2014;14(2):121-34.
4. Shapiro L, Weis WI. Structure and biochemistry of cadherins and catenins. Cold Spring Harbor perspectives in biology. 2009;1(3):a003053.
5. Leckband D, Sivasankar S. Biophysics of cadherin adhesion. Sub-cellular biochemistry. 2012;60:63-88.
6. Shan WS, Tanaka H, Phillips GR, Arndt K, Yoshida M, Colman DR, et al. Functional cis-heterodimers of N- and R-cadherins. The Journal of cell biology. 2000;148(3):579-90.
7. Halbleib JM, Nelson WJ. Cadherins in development: cell adhesion, sorting, and tissue morphogenesis. Genes & development. 2006;20(23):3199-214.
8. Stepniak E, Radice GL, Vasioukhin V. Adhesive and signaling functions of cadherins and catenins in vertebrate development. Cold Spring Harbor perspectives in biology. 2009;1(5):a002949.
9. Albergaria A, Ribeiro AS, Vieira AF, Sousa B, Nobre AR, Seruca R, et al. P-cadherin role in normal breast development and cancer. The International journal of developmental biology. 2011;55(7-9):811-22.
10. Pokutta S, Weis WI. Structure and mechanism of cadherins and catenins in cell-cell contacts. Annual review of cell and developmental biology. 2007;23:237-61.
11. Budnar S, Yap AS. A mechanobiological perspective on cadherins and the actin-myosin cytoskeleton. F1000prime reports. 2013;5:35.
12. Hiscox S, Morgan L, Green T, Nicholson RI. Src as a therapeutic target in anti-hormone/anti-growth factor-resistant breast cancer. Endocrine-related cancer. 2006;13 Suppl 1:S53-9.
13. Nollet F, Berx G, van Roy F. The role of the E-cadherin/catenin adhesion complex in the development and progression of cancer. Molecular cell biology research communications : MCBRC. 1999;2(2):77-85.
14. Riethmacher D, Brinkmann V, Birchmeier C. A targeted mutation in the mouse E-cadherin gene results in defective preimplantation development. Proceedings of the National Academy of Sciences of the United States of America. 1995;92(3):855-9.
15. Strumane K, Berx G, Van Roy F. Cadherins in cancer. Handbook of experimental pharmacology. 2004(165):69-103.

16. Birchmeier W, Behrens J. Cadherin expression in carcinomas: role in the formation of cell junctions and the prevention of invasiveness. Biochimica et biophysica acta. 1994;1198(1):11-26.

17. Hajra KM, Chen DY, Fearon ER. The SLUG zinc-finger protein represses E-cadherin in breast cancer. Cancer research. 2002;62(6):1613-8.

18. Di Croce L, Pelicci PG. Tumour-associated hypermethylation: silencing E-cadherin expression enhances invasion and metastasis. European journal of cancer. 2003;39(4):413-4.

19. Nawrocki-Raby B, Gilles C, Polette M, Bruyneel E, Laronze JY, Bonnet N, et al. Upregulation of MMPs by soluble E-cadherin in human lung tumor cells. International journal of cancer Journal international du cancer. 2003;105(6):790-5.

20. Imai K, Hirata S, Irie A, Senju S, Ikuta Y, Yokomine K, et al. Identification of a novel tumor-associated antigen, cadherin 3/P-cadherin, as a possible target for immunotherapy of pancreatic, gastric, and colorectal cancers. Clin Cancer Res. 2008;14(20):6487-95.

21. Van Marck V, Stove C, Van Den Bossche K, Stove V, Paredes J, Vander Haeghen Y, et al. P-cadherin promotes cell-cell adhesion and counteracts invasion in human melanoma. Cancer research. 2005;65(19):8774-83.

22. Paredes J, Stove C, Stove V, Milanezi F, Van Marck V, Derycke L, et al. P-cadherin is up-regulated by the antiestrogen ICI 182,780 and promotes invasion of human breast cancer cells. Cancer research. 2004;64(22):8309-17.

23. Ribeiro AS, Albergaria A, Sousa B, Correia AL, Bracke M, Seruca R, et al. Extracellular cleavage and shedding of P-cadherin: a mechanism underlying the invasive behaviour of breast cancer cells. Oncogene. 2010;29(3):392-402.

24. Zhang CC, Yan Z, Zhang Q, Kuszpit K, Zasadny K, Qiu M, et al. PF-03732010: a fully human monoclonal antibody against P-cadherin with antitumor and antimetastatic activity. Clin Cancer Res. 2010;16(21):5177-88.

25. Berx G, Van Roy F. The E-cadherin/catenin complex: an important gatekeeper in breast cancer tumorigenesis and malignant progression. Breast cancer research : BCR. 2001;3(5):289-93.

26. Cleton-Jansen AM. E-cadherin and loss of heterozygosity at chromosome 16 in breast carcinogenesis: different genetic pathways in ductal and lobular breast cancer? Breast cancer research : BCR. 2002;4(1):5-8.

27. Dykxhoorn DM, Wu Y, Xie H, Yu F, Lal A, Petrocca F, et al. miR-200 enhances mouse breast cancer cell colonization to form distant metastases. PLoS One. 2009;4(9):e7181.

28. Lou Y, Preobrazhenska O, auf dem Keller U, Sutcliffe M, Barclay L, McDonald PC, et al. Epithelial-mesenchymal transition (EMT) is not sufficient for spontaneous murine breast cancer metastasis. Dev Dyn. 2008;237(10):2755-68.

29. Ben Hamida A, Labidi IS, Mrad K, Charafe-Jauffret E, Ben Arab S, Esterni B, et al. Markers of subtypes in inflammatory breast cancer studied by immunohistochemistry: prominent expression of P-cadherin. BMC Cancer. 2008;8:28.

30. Tomlinson JS, Alpaugh ML, Barsky SH. An intact overexpressed E-cadherin/alpha,beta-catenin axis characterizes the lymphovascular emboli of inflammatory breast carcinoma. Cancer Res. 2001;61(13):5231-41.

31. Kowalski PJ, Rubin MA, Kleer CG. E-cadherin expression in primary carcinomas of the breast and its distant metastases. Breast Cancer Res. 2003;5(6):R217-22.

32. Gillett CE, Miles DW, Ryder K, Skilton D, Liebman RD, Springall RJ, et al. Retention of the expression of E-cadherin and catenins is associated with shorter survival in grade III ductal carcinoma of the breast. J Pathol. 2001;193(4):433-41.

33. Howard EM, Lau SK, Lyles RH, Birdsong GG, Umbreit JN, Kochhar R. Expression of e-cadherin in high-risk breast cancer. J Cancer Res Clin Oncol. 2005;131(1):14-8.

34. Paredes J, Albergaria A, Oliveira JT, Jeronimo C, Milanezi F, Schmitt FC. P-cadherin overexpression is an indicator of clinical outcome in invasive breast carcinomas and is associated with CDH3 promoter hypomethylation. Clin Cancer Res. 2005;11(16):5869-77.

35. Gamallo C, Moreno-Bueno G, Sarrio D, Calero F, Hardisson D, Palacios J. The prognostic significance of P-cadherin in infiltrating ductal breast carcinoma. Modern pathology : an official journal of the United States and Canadian Academy of Pathology, Inc. 2001;14(7):650-4.

36. Kovacs A, Dhillon J, Walker RA. Expression of P-cadherin, but not E-cadherin or N-cadherin, relates to pathological and functional differentiation of breast carcinomas. Mol Pathol. 2003;56(6):318-22.

37. Kovacs A, Walker RA. P-cadherin as a marker in the differential diagnosis of breast lesions. J Clin Pathol. 2003;56(2):139-41.

38. Palacios J, Benito N, Pizarro A, Suarez A, Espada J, Cano A, et al. Anomalous expression of P-cadherin in breast carcinoma. Correlation with E-cadherin expression and pathological features. Am J Pathol. 1995;146(3):605-12.

39. Paredes J, Milanezi F, Reis-Filho JS, Leitao D, Athanazio D, Schmitt F. Aberrant P-cadherin expression: is it associated with estrogen-independent growth in breast cancer? Pathol Res Pract. 2002;198(12):795-801.

40. Peralta Soler A, Knudsen KA, Salazar H, Han AC, Keshgegian AA. P-cadherin expression in breast carcinoma indicates poor survival. Cancer. 1999;86(7):1263-72.

41. Wheelock MJ, Shintani Y, Maeda M, Fukumoto Y, Johnson KR. Cadherin switching. Journal of cell science. 2008;121(Pt 6):727-35.

42. Paredes J, Correia AL, Ribeiro AS, Milanezi F, Cameselle-Teijeiro J, Schmitt FC. Breast carcinomas that co-express E- and P-cadherin are associated with p120-catenin cytoplasmic localisation and poor patient survival. Journal of clinical pathology. 2008;61(7):856-62.

43. Ribeiro AS, Sousa B, Carreto L, Mendes N, Nobre AR, Ricardo S, et al. P-cadherin functional role is dependent on E-cadherin cellular context: a proof of concept using the breast cancer model. The Journal of pathology. 2013;229(5):705-18.

44. Sarrio D, Palacios J, Hergueta-Redondo M, Gomez-Lopez G, Cano A, Moreno-Bueno G. Functional characterization of E- and P-cadherin in invasive breast cancer cells. BMC cancer. 2009;9:74.

45. Sen B, Johnson FM. Regulation of SRC family kinases in human cancers. Journal of signal transduction. 2011;2011:865819.

46. Bolos V, Gasent JM, Lopez-Tarruella S, Grande E. The dual kinase complex FAK-Src as a promising therapeutic target in cancer. OncoTargets and therapy. 2010;3:83-97.

47. Kim LC, Song L, Haura EB. Src kinases as therapeutic targets for cancer. Nature reviews Clinical oncology. 2009;6(10):587-95.

48. Xu W, Harrison SC, Eck MJ. Three-dimensional structure of the tyrosine kinase c-Src. Nature. 1997;385(6617):595-602.

49. Sanchez-Bailon MP, Calcabrini A, Gomez-Dominguez D, Morte B, Martin-Forero E, Gomez-Lopez G, et al. Src kinases catalytic activity regulates proliferation, migration and invasiveness of MDA-MB-231 breast cancer cells. Cellular signalling. 2012;24(6):1276-86.

50. Yap AS, Crampton MS, Hardin J. Making and breaking contacts: the cellular biology of cadherin regulation. Current opinion in cell biology. 2007;19(5):508-14.

51. Palacios F, Tushir JS, Fujita Y, D'Souza-Schorey C. Lysosomal targeting of E-cadherin: a unique mechanism for the down-regulation of cell-cell adhesion during epithelial to mesenchymal transitions. Molecular and cellular biology. 2005;25(1):389-402.

52. Irby RB, Yeatman TJ. Increased Src activity disrupts cadherin/catenin-mediated homotypic adhesion in human colon cancer and transformed rodent cells. Cancer research. 2002;62(9):2669-74.

53. Summy JM, Gallick GE. Src family kinases in tumor progression and metastasis. Cancer metastasis reviews. 2003;22(4):337-58.

54. Biscardi JS, Ishizawar RC, Silva CM, Parsons SJ. Tyrosine kinase signalling in breast cancer: epidermal growth factor receptor and c-Src interactions in breast cancer. Breast cancer research : BCR. 2000;2(3):203-10.

55. Hiscox S, Morgan L, Green TP, Barrow D, Gee J, Nicholson RI. Elevated Src activity promotes cellular invasion and motility in tamoxifen resistant breast cancer cells. Breast cancer research and treatment. 2006;97(3):263-74.
56. Bjorge JD, Pang A, Fujita DJ. Identification of protein-tyrosine phosphatase 1B as the major tyrosine phosphatase activity capable of dephosphorylating and activating c-Src in several human breast cancer cell lines. The Journal of biological chemistry. 2000;275(52):41439-46.
57. Belsches-Jablonski AP, Biscardi JS, Peavy DR, Tice DA, Romney DA, Parsons SJ. Src family kinases and HER2 interactions in human breast cancer cell growth and survival. Oncogene. 2001;20(12):1465-75.
58. Zhang S, Yu D. Targeting Src family kinases in anti-cancer therapies: turning promise into triumph. Trends in pharmacological sciences. 2012;33(3):122-8.
59. Kim EM, Mueller K, Gartner E, Boerner J. Dasatinib is synergistic with cetuximab and cisplatin in triple-negative breast cancer cells. The Journal of surgical research. 2013;185(1):231-9.
60. Mueller KL, Hunter LA, Ethier SP, Boerner JL. Met and c-Src cooperate to compensate for loss of epidermal growth factor receptor kinase activity in breast cancer cells. Cancer research. 2008;68(9):3314-22.
61. Behrens J, Vakaet L, Friis R, Winterhager E, Van Roy F, Mareel MM, et al. Loss of epithelial differentiation and gain of invasiveness correlates with tyrosine phosphorylation of the E-cadherin/beta-catenin complex in cells transformed with a temperature-sensitive v-SRC gene. The Journal of cell biology. 1993;120(3):757-66.
62. Coluccia AM, Benati D, Dekhil H, De Filippo A, Lan C, Gambacorti-Passerini C. SKI-606 decreases growth and motility of colorectal cancer cells by preventing pp60(c-Src)-dependent tyrosine phosphorylation of beta-catenin and its nuclear signaling. Cancer research. 2006;66(4):2279-86.
63. Lehrer S, O'Shaughnessy J, Song HK, Levine E, Savoretti P, Dalton J, et al. Activity of pp60c-src protein kinase in human breast cancer. The Mount Sinai journal of medicine, New York. 1989;56(2):83-5.
64. Verbeek BS, Vroom TM, Adriaansen-Slot SS, Ottenhoff-Kalff AE, Geertzema JG, Hennipman A, et al. c-Src protein expression is increased in human breast cancer. An immunohistochemical and biochemical analysis. The Journal of pathology. 1996;180(4):383-8.
65. Reissig D, Clement J, Sanger J, Berndt A, Kosmehl H, Bohmer FD. Elevated activity and expression of Src-family kinases in human breast carcinoma tissue versus matched non-tumor tissue. Journal of cancer research and clinical oncology. 2001;127(4):226-30.

66. Finn RS. Targeting Src in breast cancer. Annals of oncology : official journal of the European Society for Medical Oncology / ESMO. 2008;19(8):1379-86.

67. Dimri M, Naramura M, Duan L, Chen J, Ortega-Cava C, Chen G, et al. Modeling breast cancer-associated c-Src and EGFR overexpression in human MECs: c-Src and EGFR cooperatively promote aberrant three-dimensional acinar structure and invasive behavior. Cancer research. 2007;67(9):4164-72.

68. Kanda S, Miyata Y, Kanetake H, Smithgall TE. Non-receptor protein-tyrosine kinases as molecular targets for antiangiogenic therapy (Review). International journal of molecular medicine. 2007;20(1):113-21.

69. Petreaca ML, Yao M, Liu Y, Defea K, Martins-Green M. Transactivation of vascular endothelial growth factor receptor-2 by interleukin-8 (IL-8/CXCL8) is required for IL-8/CXCL8-induced endothelial permeability. Molecular biology of the cell. 2007;18(12):5014-23.

70. Werdich XQ, Penn JS. Src, Fyn and Yes play differential roles in VEGF-mediated endothelial cell events. Angiogenesis. 2005;8(4):315-26.

71. Missbach M, Altmann E, Widler L, Susa M, Buchdunger E, Mett H, et al. Substituted 5,7-diphenyl-pyrrolo[2,3d]pyrimidines: potent inhibitors of the tyrosine kinase c-Src. Bioorganic & medicinal chemistry letters. 2000;10(9):945-9.

72. Susa M, Teti A. Tyrosine kinase src inhibitors: potential therapeutic applications. Drug news & perspectives. 2000;13(3):169-75.

73. Maly DJ, Choong IC, Ellman JA. Combinatorial target-guided ligand assembly: identification of potent subtype-selective c-Src inhibitors. Proceedings of the National Academy of Sciences of the United States of America. 2000;97(6):2419-24.

74. Neet K, Hunter T. Vertebrate non-receptor protein-tyrosine kinase families. Genes to cells : devoted to molecular & cellular mechanisms. 1996;1(2):147-69.

75. Thomas SM, Brugge JS. Cellular functions regulated by Src family kinases. Annual review of cell and developmental biology. 1997;13:513-609.

76. Steinberg M. Dasatinib: a tyrosine kinase inhibitor for the treatment of chronic myelogenous leukemia and philadelphia chromosome-positive acute lymphoblastic leukemia. Clinical therapeutics. 2007;29(11):2289-308.

77. Gnoni A, Marech I, Silvestris N, Vacca A, Lorusso V. Dasatinib: an anti-tumour agent via Src inhibition. Current drug targets. 2011;12(4):563-78.

78. Karim SA, Creedon H, Patel H, Carragher NO, Morton JP, Muller WJ, et al. Dasatinib inhibits mammary tumour development in a genetically engineered mouse model. The Journal of pathology. 2013;230(4):430-40.

79. Nautiyal J, Majumder P, Patel BB, Lee FY, Majumdar AP. Src inhibitor dasatinib inhibits growth of breast cancer cells by modulating EGFR signaling. Cancer letters. 2009;283(2):143-51.
80. Kuznetsova TG, Starodubtseva MN, Yegorenkov NI, Chizhik SA, Zhdanov RI. Atomic force microscopy probing of cell elasticity. Micron. 2007;38(8):824-33.
81. Bischoff G, Engineering ESf, Medicine. Micro- and Nanostructures of Biological Systems: Shaker Verlag GmbH; 2005.
82. Fotiadis D, Scheuring S, Muller SA, Engel A, Muller DJ. Imaging and manipulation of biological structures with the AFM. Micron. 2002;33(4):385-97.
83. Alexander S, Hellemans L, Marti O, Schneir J, Elings V, Hansma PK, et al. An atomic‐resolution atomic‐force microscope implemented using an optical lever. Journal of Applied Physics. 1989;65(1):164-7.
84. Santos NC, Castanho MA. An overview of the biophysical applications of atomic force microscopy. Biophysical chemistry. 2004;107(2):133-49.
85. Taubenberger A, Cisneros DA, Friedrichs J, Puech PH, Muller DJ, Franz CM. Revealing early steps of alpha2beta1 integrin-mediated adhesion to collagen type I by using single-cell force spectroscopy. Molecular biology of the cell. 2007;18(5):1634-44.
86. Heymann JB, Pfeiffer M, Hildebrandt V, Kaback HR, Fotiadis D, Groot B, et al. Conformations of the rhodopsin third cytoplasmic loop grafted onto bacteriorhodopsin. Structure. 2000;8(6):643-53.
87. Muller DJ, Fotiadis D, Scheuring S, Muller SA, Engel A. Electrostatically balanced subnanometer imaging of biological specimens by atomic force microscope. Biophysical journal. 1999;76(2):1101-11.
88. Valle M, Valpuesta JM, Carrascosa JL, Tamayo J, Garcia R. The interaction of DNA with bacteriophage phi 29 connector: a study by AFM and TEM. Journal of structural biology. 1996;116(3):390-8.
89. Viani MB, Pietrasanta LI, Thompson JB, Chand A, Gebeshuber IC, Kindt JH, et al. Probing protein-protein interactions in real time. Nature structural biology. 2000;7(8):644-7.
90. Cheung CL, Hafner JH, Lieber CM. Carbon nanotube atomic force microscopy tips: direct growth by chemical vapor deposition and application to high-resolution imaging. Proceedings of the National Academy of Sciences of the United States of America. 2000;97(8):3809-13.
91. Dufrene YF, Pelling AE. Force nanoscopy of cell mechanics and cell adhesion. Nanoscale. 2013;5(10):4094-104.
92. Carvalho FA, Santos NC. Atomic force microscopy-based force spectroscopy--biological and biomedical applications. IUBMB life. 2012;64(6):465-72.

93. Cluzel P, Lebrun A, Heller C, Lavery R, Viovy JL, Chatenay D, et al. DNA: an extensible molecule. Science. 1996;271(5250):792-4.

94. Shi X, Zhang X, Xia T, Fang X. Living cell study at the single-molecule and single-cell levels by atomic force microscopy. Nanomedicine. 2012;7(10):1625-37.

95. Heinz WF, Hoh JH. Spatially resolved force spectroscopy of biological surfaces using the atomic force microscope. Trends in biotechnology. 1999;17(4):143-50.

96. Docheva D, Padula D, Popov C, Mutschler W, Clausen-Schaumann H, Schieker M. Researching into the cellular shape, volume and elasticity of mesenchymal stem cells, osteoblasts and osteosarcoma cells by atomic force microscopy. Journal of cellular and molecular medicine. 2008;12(2):537-52.

97. Wirtz D, Konstantopoulos K, Searson PC. The physics of cancer: the role of physical interactions and mechanical forces in metastasis. Nature reviews Cancer. 2011;11(7):512-22.

98. Casuso I, Rico F, Scheuring S. Biological AFM: where we come from--where we are--where we may go. Journal of molecular recognition : JMR. 2011;24(3):406-13.

99. Lekka M, Laidler P, Gil D, Lekki J, Stachura Z, Hrynkiewicz AZ. Elasticity of normal and cancerous human bladder cells studied by scanning force microscopy. European biophysics journal : EBJ. 1999;28(4):312-6.

100. Gimzewski JK, Joachim C. Nanoscale science of single molecules using local probes. Science. 1999;283(5408):1683-8.

101. Leckband D. Force as a probe of membrane protein structure and function. Current opinion in structural biology. 2001;11(4):433-9.

102. Wojcikiewicz EP, Zhang X, Moy VT. Force and Compliance Measurements on Living Cells Using Atomic Force Microscopy (AFM). Biological procedures online. 2004;6:1-9.

103. Franz CM, Puech PH. Atomic Force Microscopy: A Versatile Tool for Studying Cell Morphology, Adhesion and Mechanics. Cellular and Molecular Bioengineering. 2008;1(4):289-300.

104. Evans EA, Calderwood DA. Forces and bond dynamics in cell adhesion. Science. 2007;316(5828):1148-53.

105. Hinterdorfer P, Baumgartner W, Gruber HJ, Schilcher K, Schindler H. Detection and localization of individual antibody-antigen recognition events by atomic force microscopy. Proceedings of the National Academy of Sciences of the United States of America. 1996;93(8):3477-81.

106. Muller DJ, Helenius J, Alsteens D, Dufrene YF. Force probing surfaces of living cells to molecular resolution. Nature chemical biology. 2009;5(6):383-90.

107. Bershadsky A, Kozlov M, Geiger B. Adhesion-mediated mechanosensitivity: a time to experiment, and a time to theorize. Current opinion in cell biology. 2006;18(5):472-81.
108. Sun M, Northup N, Marga F, Huber T, Byfield FJ, Levitan I, et al. The effect of cellular cholesterol on membrane-cytoskeleton adhesion. Journal of cell science. 2007;120(Pt 13):2223-31.
109. Plodinec M, Loparic M, Monnier CA, Obermann EC, Zanetti-Dallenbach R, Oertle P, et al. The nanomechanical signature of breast cancer. Nature nanotechnology. 2012;7(11):757-65.
110. Hogan C, Dupre-Crochet S, Norman M, Kajita M, Zimmermann C, Pelling AE, et al. Characterization of the interface between normal and transformed epithelial cells. Nature cell biology. 2009;11(4):460-7.
111. Suresh S. Biomechanics and biophysics of cancer cells. Acta biomaterialia. 2007;3(4):413-38.
112. Cross SE, Jin YS, Rao J, Gimzewski JK. Nanomechanical analysis of cells from cancer patients. Nature nanotechnology. 2007;2(12):780-3.
113. Yamazaki D, Kurisu S, Takenawa T. Regulation of cancer cell motility through actin reorganization. Cancer science. 2005;96(7):379-86.
114. Discher DE, Janmey P, Wang YL. Tissue cells feel and respond to the stiffness of their substrate. Science. 2005;310(5751):1139-43.
115. Paszek MJ, Zahir N, Johnson KR, Lakins JN, Rozenberg GI, Gefen A, et al. Tensional homeostasis and the malignant phenotype. Cancer cell. 2005;8(3):241-54.
116. Puech PH, Poole K, Knebel D, Muller DJ. A new technical approach to quantify cell-cell adhesion forces by AFM. Ultramicroscopy. 2006;106(8-9):637-44.
117. Pillet F, Chopinet L, Formosa C, Dague E. Atomic Force Microscopy and pharmacology: from microbiology to cancerology. Biochimica et biophysica acta. 2014;1840(3):1028-50.
118. Huang C, Jin H, Song B, Zhu X, Zhao H, Cai J, et al. The cytotoxicity and anticancer mechanisms of alterporriol L, a marine bianthraquinone, against MCF-7 human breast cancer cells. Applied microbiology and biotechnology. 2012;93(2):777-85.
119. Kim KS, Cho CH, Park EK, Jung MH, Yoon KS, Park HK. AFM-detected apoptotic changes in morphology and biophysical property caused by paclitaxel in Ishikawa and HeLa cells. PloS one. 2012;7(1):e30066.
120. Targosz-Korecka M, Biedron R, Szczygiel AM, Brzezinka G, Szczerbinski J, Zuk A. Stiffness changes of tumor HEp2 cells correlates with the inhibition and release of TRAIL-induced apoptosis pathways. Journal of molecular recognition : JMR. 2012;25(5):299-308.

121. Hoh JH, Schoenenberger CA. Surface morphology and mechanical properties of MDCK monolayers by atomic force microscopy. Journal of cell science. 1994;107 (Pt 5):1105-14.

122. Suresh S. Nanomedicine: elastic clues in cancer detection. Nature nanotechnology. 2007;2(12):748-9.

123. Wijnhoven BP, Dinjens WN, Pignatelli M. E-cadherin-catenin cell-cell adhesion complex and human cancer. The British journal of surgery. 2000;87(8):992-1005.

124. Bukholm IK, Nesland JM, Karesen R, Jacobsen U, Borresen-Dale AL. E-cadherin and alpha-, beta-, and gamma-catenin protein expression in relation to metastasis in human breast carcinoma. The Journal of pathology. 1998;185(3):262-6.

125. Nam S, Kim D, Cheng JQ, Zhang S, Lee JH, Buettner R, et al. Action of the Src family kinase inhibitor, dasatinib (BMS-354825), on human prostate cancer cells. Cancer research. 2005;65(20):9185-9.